

Fused inverse-normal method for integrated differential expression analysis of RNA-seq data

Birbal Prasad¹ and Xinzhong Li^{1*}

¹National Horizons Centre, School of Health and Life Sciences, Teesside University, Darlington, DL1 1HG, UK. Email: B.Prasad@tees.ac.uk; X.Li@tees.ac.uk

*Correspondence: Email: X.Li@tees.ac.uk, Phone: [+44-01642738451](tel:+44-01642738451)

Abstract

Background: Use of next-generation sequencing technologies to transcriptomics (RNA-seq) for gene expression profiling has found widespread application in studying different biological conditions including cancers. However, RNA-seq experiments are still small sample size experiments due to the cost. Recently, an increased focus has been on meta-analysis methods for integrated differential expression analysis for exploration of potential biomarkers. In this study, we propose a p-value combination method for meta-analysis of multiple related RNA-seq studies that accounts for sample size of a study and direction of expression of genes in individual studies.

Results: The proposed method generalizes the inverse-normal method without increase in computational complexity and does not pre- or post-hoc filter genes that have conflicting direction of expression in different studies. Thus, the proposed method, as compared to the inverse-normal, has better potential for the discovery of differentially expressed genes (DEGs) with potentially conflicting differential signals from multiple studies related to disease. We demonstrated the use of the proposed method in detection of biologically relevant DEGs in glioblastoma (GBM), the most aggressive brain cancer. Our approach notably enabled the identification of over-expression in GBM compared to healthy controls of the oncogene *RAD51*, which has recently been shown to be a target for inhibition to enhance radiosensitivity of GBM cells during treatment. Pathway analysis identified multiple aberrant GBM related pathways as well as novel regulators such as *TCF7L2* and *MAPT* as important upstream regulators in GBM.

Conclusions: The proposed meta-analysis method generalizes the existing inverse-normal method by providing a way to establish differential expression status for genes with conflicting direction of expression in individual RNA-seq studies. Hence, leading to further exploration of them as potential biomarkers for the disease.

Keywords: Meta-analysis, RNA-seq, glioblastoma, differential expression

Background

RNA sequencing (RNA-seq) technologies are now increasingly considered for whole transcriptome gene expression quantification studies as compared to traditional microarray technologies due to its high technical reproducibility and greater resolution [1]. Over the last decade, it has found widespread application in studying different biological conditions including cancers. For instance, sequencing data archived on The Cancer Genome Atlas (<https://portal.gdc.cancer.gov/>) have been used in a number of studies to explore potential biomarkers and mechanisms in oncogenesis [2][3]. Despite its advantages and few large RNA-seq datasets [4][5], RNA-seq experiments are still small sample size experiments because of its high cost. This leads to a problem of reduced statistical power in studies such as differential expression analysis where thousands of genes are studied at a time but only have tens to

hundreds of samples. Combination of data or results from multiple independent but related studies (referred to as meta-analysis) have been widely used to increase available sample size and consequently the statistical power to obtain a precise estimate of gene expression differentials [6][7]. In the context of differential expression analysis, several different meta-analysis approaches have been proposed for integrating microarray studies [8][9] and some of them have later been adapted for RNA-seq data [10][11].

For microarray gene expression studies, apart from vote-counting and direct merging of datasets, meta-analysis methods can mainly be classified into three types based on the combined statistic [7]. First are methods based on effect sizes combination in which a combined effect (for instance, strength of differential expression between two conditions for a gene) is obtained based on the calculated effect sizes and its variance where two possible models namely, fixed and random effects model are used to obtain the combined effect [12]. Second are approaches based on integration of p-values obtained from per-study analysis into a single combined p-value per gene [13]. Lastly, are approaches based on rank combination which are non-parametric and allow for integration of studies based on a statistic that can be ordered, e.g., fold change of a gene [14]. However, RNA-seq data are counts data, i.e., normalized number of sequenced reads within a certain gene or transcript, unlike the microarray data which are continuous, e.g., normalized signal intensity of image [15]. Hence, the methods initially proposed for microarray data are not suited to be applied directly to RNA-seq data in many cases [10].

In case of RNA-seq data, Poisson or Negative-Binomial distributions are typically used to model gene counts [16]. Kulinskaya et al. (2008) [17] described an effect-size combination method using an Anscombe transformation of Poisson distributed data. However, as highlighted by Rau et al. (2014) [10], this effect-size combination approach is not appropriate for RNA-seq data due to over-dispersion among biological replicates and presence of zero-inflation. Rau et al. (2014) considered two p-value combination methods, namely Fisher and inverse normal (IN) or Stouffer's methods, previously proposed and used for meta-analysis of microarray studies [8][9][13] and demonstrated how these can be adapted in RNA-seq data analysis. Their results illustrated that Fisher and IN methods were very similar to each other in terms of performance but were better than the global and per-study differential analysis [10]. These two (Fisher and IN) p-value combination approaches have been implemented in several R packages, e.g., metaRNASeq [10], metaseqR [18] and metaSeq [19] and are most widely used methods due to its statistical simplicity and ease of direct application for meta-analysis of RNA-seq studies for differential expression.

Among all the existing meta-analysis methods for RNA-seq data discussed above, only few of the p-value combination methods (e.g., IN and PANDORA p-value [18]) allow for incorporation of information regarding the number of replicates in different studies to be combined through specification of a set of weights. However, information related to the direction of expression (up- or down-regulated) of a gene across different studies is not accounted for or included in any of these meta-analysis methods for RNA-seq data. Under- and over-expressed genes are analysed together and genes exhibiting conflicting direction of expression across studies are either removed prior to meta-analysis or are suggested to be identified and removed post-hoc [10][11]. Hence, no conclusion can be drawn with regards to differential expression for the genes that have conflicting direction of expression across different studies. Given that a significant proportion of genes may exhibit conflicting direction of expression across different gene expression studies [20], particularly when more and more

RNA-seq data are publicly available and included into integration, emphasis is warranted on including this important prior information in a meta-analysis setting.

Recently, importance of inclusion of direction of expression information for genes in RNA-seq meta-analysis has been recognized leading to a generalization of some existing p-value combination methods such as Fisher method and Bayesian Hierarchical Model [21][22][23]. However, these generalizations come at a cost of increased statistical and computational complexity which discourages their widespread application to transcriptomic studies. In this study, we aimed to develop a new approach for integrated differential meta-analysis of RNA-seq data which accounts for both the sample size and direction of gene regulation in each study. The proposed approach leads to a generalization of the IN method without introducing additional cost and hence is simple and intuitive for real data application. First, we propose a modified inverse-normal (MIN) approach for p-value combination and assess its performance by comparing it with the IN method based on an extensive simulation study. Next, to overcome the conservative nature of MIN method, we further propose a fused inverse normal (FIN) method for p-value combination and assess its performance by comparing it to IN and MIN methods in a simulation study. Then an application to a set of real glioblastoma (GBM, the most aggressive type of brain cancer) studies has been conducted. Moreover, we assessed the relevance of the identified differentially expressed genes (DEGs) for GBM by using Ingenuity Pathway Analysis (IPA, www.qiagen.com/ingenuity) for pathway analysis and upstream regulator analysis.

Methods

Let y_{gcrs} be the observed count for gene g ($g = 1, 2, \dots, G$) in condition c ($c = 1, 2$) of biological replicate r ($r = 1, 2, \dots, R_{cs}$) in study s ($s = 1, 2, \dots, S$). For an integrated differential analysis of gene expression across multiple studies, we first conducted the differential expression analysis within a given study s using edgeR package (version 3.26.5) in R version 3.6.0 [24] with likelihood ratio test as the test for differential expression. Let p_{gs} be the raw p-value for per-gene and per-study obtained using the individual differential expression analysis within a given study s for gene g . The null hypothesis tested in the individual differential analysis is that the gene is non-differentially expressed in the particular study. For notational convenience, the notations similar to the ones used in Rau et al. (2014) [10] were adopted in this study.

Modified inverse-normal method

Let B_{gs} be a Bernoulli random variable which takes values 1 and -1 when a gene g is over and under expressed respectively in a study s . A gene can be assessed as over- or under-expressed based on the fold change values (>1 or <1) of the gene in a study. Then, for a gene g , we define a combined statistic

$$N_g = \sum_{s=1}^S w_s B_{gs} |\Phi^{-1}(1 - p_{gs})| \quad (1)$$

where w_s are a set of study specific weights described by Marot and Mayer [25] as follows:

$$w_s = \sqrt{\frac{\sum_c R_{cs}}{\sum_k \sum_c R_{ck}}} \quad (2)$$

Here, $\sum_c R_{cs}$ is the total number of biological replicates in a study s for all condition c and $\sum_k \sum_c R_{ck}$ indicates the total number of biological replicates in all studies. Moreover, N_g can be considered as a weighted z-score. An advantage of this weighting criteria is that larger weights are attributed to studies with larger sample sizes. Φ is the standard normal cumulative distribution function and p_{gs} is the raw p-value obtained for gene g by differential analysis for study s .

It is assumed that p_{gs} are uniformly distributed under the null hypothesis and $\Phi^{-1}(1 - p_{gs})$ is standard normal in the above formula (1), but this assumption of p_{gs} is not automatically satisfied when dealing with RNA-seq data [10]. However, filtering of very low expressed genes in each study results in p-values which are roughly uniformly distributed under the null hypothesis [10]. Then, we have that $B_{gs}|\Phi^{-1}(1 - p_{gs})| \sim N(0, 1)$ (see Theorem 1).

Theorem 1: Let X and Y be two independent random variables where $X \sim N(0, 1)$ and Y is a Bernoulli random variable taking values 1 and -1 . Then, $Z = Y|X|$ is standard normal distributed.

Proof: Using the first principle,

$$\begin{aligned} \mathbb{P}[Y|X| \leq t] &= \mathbb{P}[Y = 1, |X| \leq t] + \mathbb{P}[Y = -1, -|X| \leq t] \\ &= \frac{1}{2}\mathbb{P}[|X| \leq t] + \frac{1}{2}\mathbb{P}[|X| \geq -t] \end{aligned} \quad (3)$$

Now, if $t < 0$, the RHS of (3) becomes $\frac{1}{2}\mathbb{P}[|X| \geq t]$. By symmetry of the normal distribution, we have

$$\mathbb{P}[Y|X| \leq t] = \mathbb{P}[X < t] = \Phi(t)$$

where Φ is the cumulative distribution function of standard normal.

For $t \geq 0$, the RHS of (3) becomes $\frac{1}{2}\mathbb{P}[|X| \leq t] + \frac{1}{2}$. Hence, by symmetry of the normal distribution, we have

$$\mathbb{P}[Y|X| \leq t] = \mathbb{P}[X \in [0, t]] + \frac{1}{2} = \mathbb{P}[X \leq t] = \Phi(t)$$

Thus, $Z \sim N(0, 1)$. ■

Hence, N_g in equation (1) is a linear combination of independent standard normal variables. Thus, is also standard normal. A two-sided test can then be performed with H_0 being that the gene g is not differentially expressed between two conditions (case vs control) and combined p-value is given by $(p_g = \mathbb{P}(|z| \geq N_g))$, i.e.

$$p_g = 2[1 - \Phi(|N_g|)]$$

A correction for multiple testing to control the false discovery rate (FDR) at a desired level α can be done by Benjamini-Hochberg (BH) approach [26].

Simulation study: MIN and IN comparison

To investigate the performance and compare the MIN method with state-of-the-art p-value combination method (IN with post-hoc filtering), we performed a simulation study. An extensive set of RNA-seq data was generated using the negative binomial distribution for the counts y_{gcrs} and method described in Rau et al. (2014) [10] (see Supplementary 1, section: Simulation study model). Parameters for the simulation study were estimated from a real RNA-seq dataset for Alzheimer's disease (AD) study downloaded from Gene Expression Omnibus (GEO, <https://www.ncbi.nlm.nih.gov/geo/>) [27] with accession number GSE125583 which contains data for 219 AD patients and 70 normal control subjects. The method used for estimation of mean and dispersion parameters from GSE125583 were as described in Rau et al. (2014) with BH p-value < 0.05 being used to classify a gene as a DEG. This dataset was chosen as it has considerable number of samples for both biological conditions, namely case and control. Simulation settings for inter-study variability parameter (σ), number of samples per condition and number of studies have been detailed in Table 1. The inter-study variability parameter represents the amount of variability between the studies considered for meta-analysis. In practice, the observed variability between human data studies is considerable

($\sigma \sim 0.5$) [10]. We chose two different values of σ (0.15 and 0.5) to represent small and large amount of inter-study variability respectively. For each setting described in Table 1, 100 independent trials were considered.

Setting	σ	No. of studies	No. of replicates (case, control)	AUC (MIN, IN, FIN)	Std. dev (MIN, IN, FIN)
1	0.15	3	(10, 10) (15, 10) (12, 16)	0.886, 0.920, 0.920	0.005, 0.003, 0.003
2	0.15	5	(10, 10) (15, 10) (12, 16) (14, 12) (20, 20)	0.953, 0.970, 0.970	0.005, < 0.001, 0.001
3	0.5	3	(10, 10) (15, 10) (12, 16)	0.950, 0.965, 0.966	0.004, 0.005, 0.005
4	0.5	5	(10, 10) (15, 10) (12, 16) (14, 12) (20, 20)	0.957, 0.977, 0.977	0.005, 0.005, 0.005

Table 1. Simulation settings for inter-study variability parameter (σ), number of studies and number of replicates per study. Area under the ROC curves (AUC) for IN, MIN and FIN methods computed using 100 trials for each simulation setting.

For each simulation setting, individual p-values obtained from differential expression analysis using edgeR were combined using both MIN and IN methods. A gene was considered differentially expressed if the BH adjusted combined p-value (FDR) < 0.05. Based on area under the ROC curves (AUC) (Table 1, Figure 1), both meta-analysis methods performed well in terms of detection power in identifying DEGs under all simulation settings. For both low ($\sigma = 0.15$) and high ($\sigma = 0.5$) inter-study variability we observed that the MIN method was more conservative (AUC was smaller than IN) than the IN method. However, as the inter-study variability and the number of studies to be combined increased, both meta-analysis methods were found to have comparable performance (Figure 1c-1d). Although slightly conservative in its performance with respect to the IN approach, MIN method has the advantage of using direction of expression information leading to identification of DEGs among genes with conflicting direction of expression across studies. The conservative behaviour of the MIN method can be attributed to the fact that a two-sided hypothesis testing is performed as compared to a one-sided test on right-hand tail of the distribution in case of IN method. Hence, next we proposed the FIN method as a mixture of IN and MIN methods to circumvent the issue of conservativeness of MIN method.

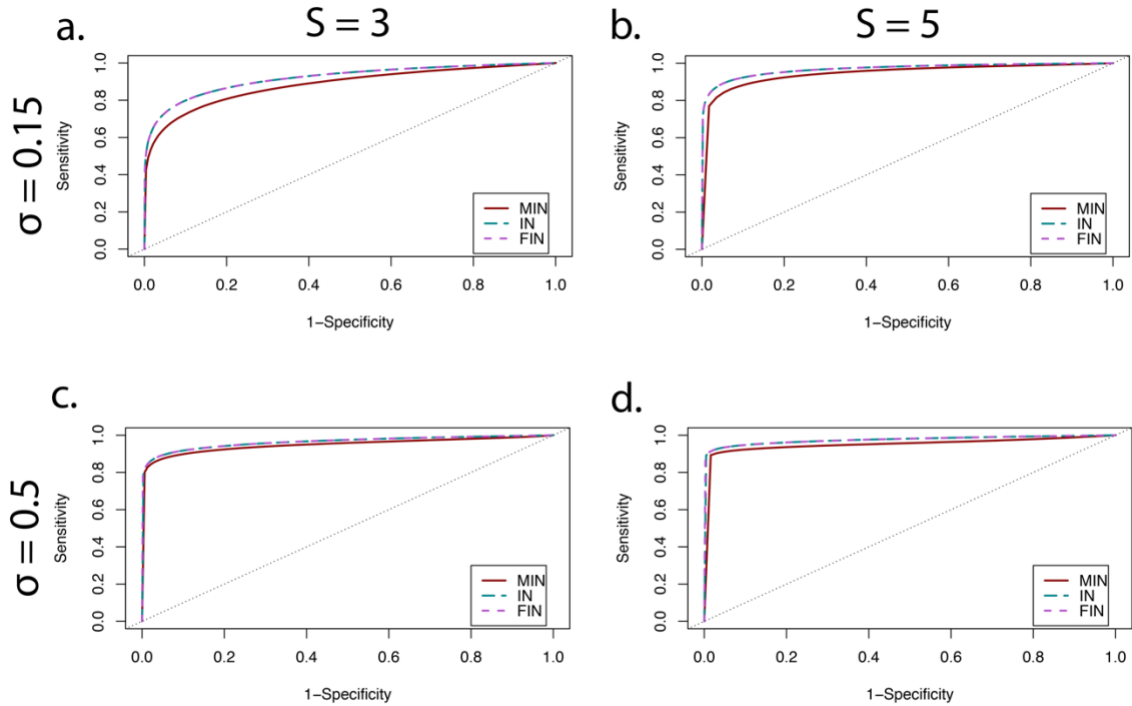


Figure 1. Performance comparison of modified inverse-normal, inverse-normal and fused inverse-normal methods. Plots of receiver operating characteristics (ROC) curves averaged over 100 trials for each simulation setting. Simulation settings are represented by rows (from top to bottom): corresponding to low ($\sigma = 0.15$) and high ($\sigma = 0.5$) inter-study variability and columns (from left to right): corresponding to 3 ($S=3$) and 5 studies ($S=5$) combined. The red, turquoise and magenta ROC curves represent the modified inverse-normal, inverse-normal and fused inverse-normal methods respectively.

As expected, with increase in inter-study variability and number of studies to be combined, the number of genes with mismatched direction of expression was significantly higher (see Supplementary 1: Table 1). We also note that the FDR for all simulation settings was controlled well below 5% threshold (Figure 2a). In terms of uniquely identified DEGs by the MIN method as compared to IN method, the proportion of true positives (TP) was higher than 80% (Figure 2b) in all simulation settings. A large proportion of TPs among the unique DEGs identified by the MIN method indicates that the MIN approach can lead to DEGs that are biologically relevant to a disease in a real application. Moreover, as the inter-study variability, number of studies or both increased, there was an increase in the number of uniquely identified DEGs by the MIN method and proportion of TPs among them (Figure 2b). More importantly, a high percentage of these unique DEGs (>75% in all settings) were observed to have the true direction of expression (Figure 2c) suggesting that a significantly high percentage of uniquely identified DEGs by the MIN method in real data applications will have true direction of expression as their effective direction of expression. The effective observed direction of expression was determined by the sign of N_g as defined in equation (1).

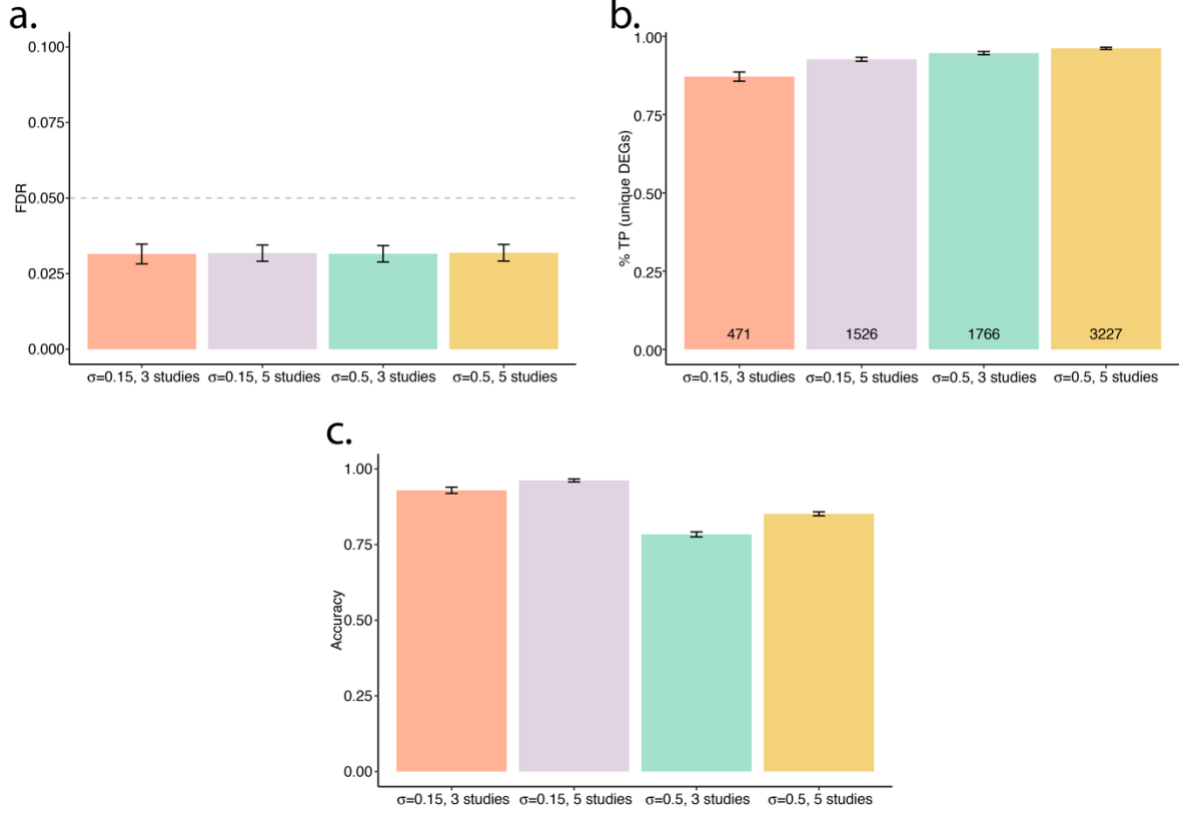


Figure 2. Characteristics of modified inverse-normal method. **a).** False discovery rates for modified inverse-normal method for all simulation settings. **b).** Proportion of true-positives (TPs) among unique differentially expressed genes (DEGs) identified by modified inverse-normal (MIN) method as compared to inverse-normal (IN) method. **c).** Proportion of unique DEGs (MIN) with the observed effective direction of expression as the true direction of expression.

Fused inverse-normal method

To address the conservative nature of MIN method, we propose a mixture method which is a mixture of IN and MIN method for integrated differential analysis. In contrast to formula (1) we define N_g as follows:

$$N_g = \begin{cases} \sum_{s=1}^S w_s \Phi^{-1}(1 - p_{g_s}), & \text{if } g \text{ has same direction of expression across } s \\ \sum_{s=1}^S w_s B_{g_s} |\Phi^{-1}(1 - p_{g_s})|, & \text{otherwise} \end{cases} \quad (4)$$

Here, w_s , Φ and B_{g_s} have their usual meaning as described previously. As N_g follows a standard normal distribution given the assumption that p_{g_s} is uniformly distributed under the null hypothesis, a one-sided test on the right-hand tail of the distribution (as proposed in [10]) can be performed for genes with same direction of expression across studies. For the genes with conflicting direction of expression across studies, a two-sided test can be performed. H_0 being the same in both the cases. Multiple testing correction to control the overall FDR can then be carried out using the BH method. A detailed interpretation of the FIN model in terms of differential expression of a gene and its direction of expression in individual studies can be found in Supplementary 1.

Simulation study: FIN, IN and MIN comparison

In addition to the simulation study for comparing MIN with IN method, we assess and compare the performance of FIN method to that of IN and MIN methods by using the same simulated

data and settings described in Table 1. Based on AUC (Table 1, Figure 1), FIN performed similar or better than IN method and had better performance than MIN under all simulation settings. As with MIN, FIN method also has the advantage of using direction of expression information and hence identified DEGs among genes with conflicting direction of expression in contrast with IN method. More importantly, we observed that FIN significantly improved detection power for true DE genes with concordant differential expression patterns across studies as compared to MIN method and does not lead to increased number of false positive detections overall (Figure 3a).

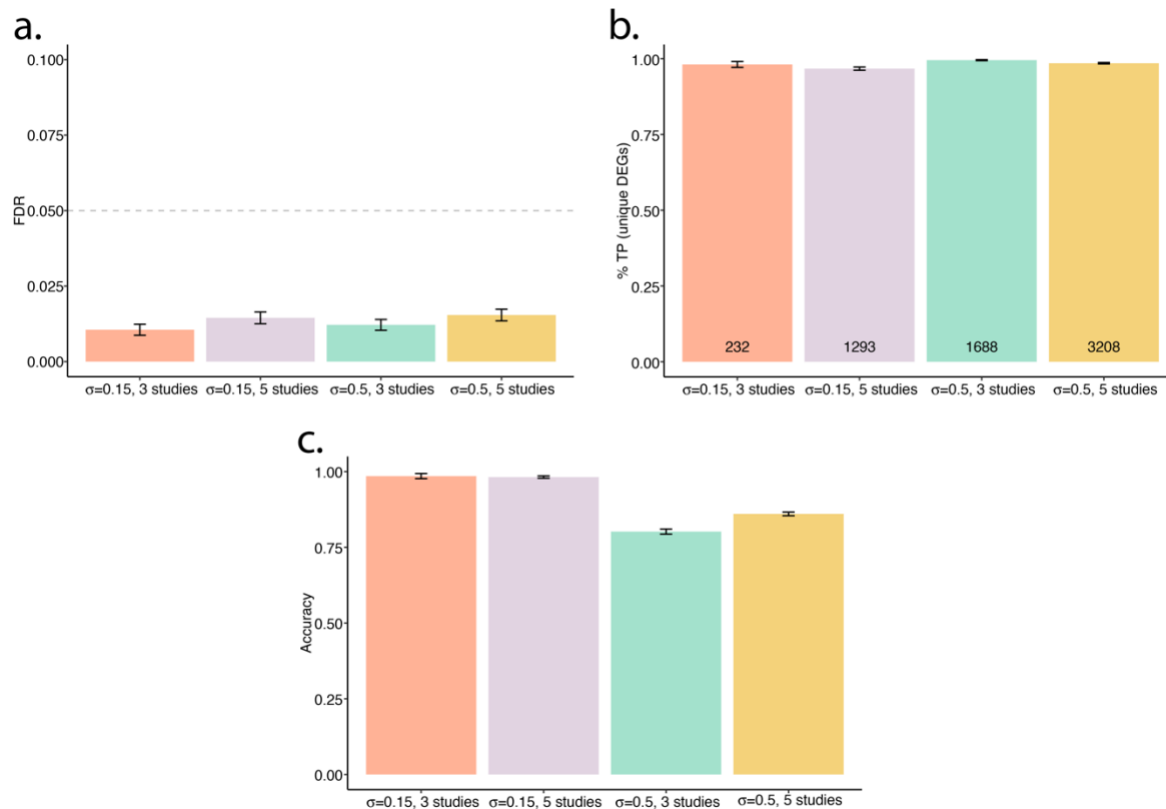


Figure 3. Characteristics of fused inverse-normal method. a). False discovery rates for fused inverse-normal method for all simulation settings. **b).** Proportion of true-positives (TPs) among unique differentially expressed genes (DEGs) identified by fused inverse-normal (FIN) method as compared to inverse-normal (IN) method. **c).** Proportion of unique DEGs (FIN) with the observed effective direction of expression as the true direction of expression.

As compared to IN, the proportion of TPs among the uniquely identified DEGs by FIN method was higher than 90% (Figure 3b) indicating that FIN method can lead to DEGs that are biologically relevant to a disease in a real application. Similar to MIN, as the inter-study variability, number of studies or both increased, there was an increase in the number of uniquely identified DEGs by the FIN method as compared to IN method and proportion of TPs among them (Figure 3b). In addition, a high percentage of these unique DEGs (>80% in all settings) were observed to have the true direction of expression (Figure 3c) suggesting that a significantly high percentage of uniquely identified DEGs by the FIN method in real data applications will have true direction of expression as their effective direction of expression. The effective observed direction of expression was determined by the sign of N_g for genes with conflicting direction of expression across studies. In case of same direction of expression of a

gene across studies, the consistent direction of expression was kept as the effective direction of expression.

Application to brain cancer data

To demonstrate how the MIN and FIN method can be adapted in practice for differential meta-analysis of RNA-seq data and compare it with IN method, an application to real GBM studies has been conducted.

Data description

GBM RNA-seq datasets were searched in GEO (<https://www.ncbi.nlm.nih.gov/geo/>) and TCGA databases (<https://portal.gdc.cancer.gov/>). Datasets were selected based on a selection criterion that at least 3 GBM patients and 3 normal tissue samples are available for analysis. Three different GBM RNA-seq datasets, two from GEO (with accession ID: GSE123892 and GSE151352) and one from TCGA (TCGA-GBM) matched our selection criteria and were considered for analysis (for details, see Table 2). Raw gene or transcript counts data (where available) was directly downloaded for TCGA-GBM and GSE123892 datasets. For GSE151352, raw FASTQ files were downloaded and processed using Galaxy web platform via the European UseGalaxy server (<https://usegalaxy.eu/>) [28] to obtain raw counts. The quality of the raw reads was assessed (using FastQC) and the specified adapter sequence ATCACCGACTGCCCATAGAGAGGCTGAGAC was removed with Cutadapt (version 1.16) [29]. The parameters used for this step were the parameters provided by the submitter of the dataset on GEO. The adapter trimmed reads were aligned to the reference genome (GRCh37.p13) using sequence aligner RNA STAR (Galaxy version 2.7.5b) [30] where other parameters used were default settings. Following alignment, the generated BAM files were processed using the featureCounts tool (Galaxy version 1.6.4+galaxy2) to get raw counts for each RNA-seq data sample. More details of the processing pipeline used for GSE151352 can be found in Supplementary 1: Figure 1.

Datasets	No. of replicates (Cases/Normal)	No. of genes (after filtering)	Up DEGs	Down DEGs
GSE123892	4/3	15024	1914	1837
GSE151352	12/12	12916	670	1545
TCGA-GBM	160/5	17943	3746	3183

Table 2. Information about GBM RNA-seq datasets used for integrated analysis using different p-value combination methods in our study. Up and down DEGs refer to the up and down-regulated DEGs obtained in per-study differential analysis.

Per-study differential expression analysis

Each of these datasets were processed separately for quality control and differential expression analysis using edgeR package (version 3.26.5) in R. Raw counts data (transcript) were annotated by mapping Ensembl IDs to Entrez Gene IDs and gene symbols (org.Hs.eg.db package, version 3.8.2 in R [31]). Ensembl IDs with no Entrez ID mapping were filtered out. For those with multiple matchings, the one with highest aggregated count was selected. Counts per million (CPM) threshold was carefully selected to reduce the number of low expressed transcripts. We removed a transcript if number of samples equal to or more than the minimum number of samples in a condition had less than 0.85 CPM for that transcript. Although subjective, this choice of threshold seems to work well for the uniform distribution assumption for the p-values under H_0 . Only genes left after low expression filtering were considered for

individual differential expression analysis in order to satisfy the uniformity assumption on p-values under the null hypothesis (Figure 4a).

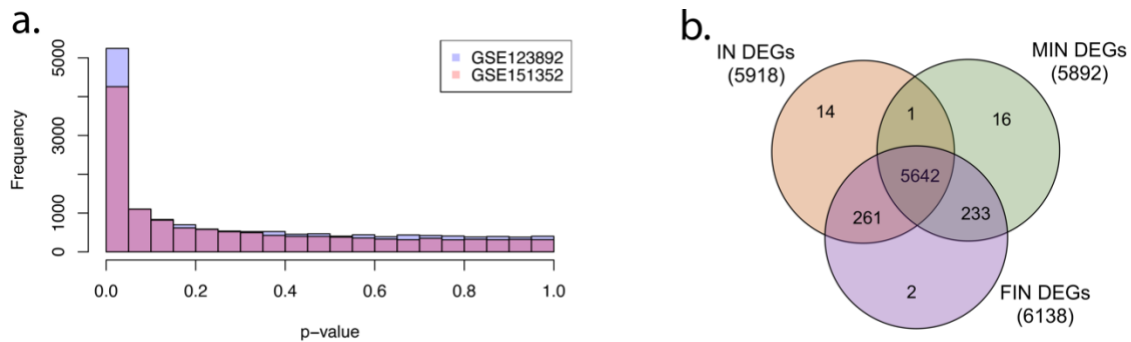


Figure 4. Comparison of results from meta-analysis methods. a). Histograms of raw p-values obtained from per-study differential analysis of GSE123892 and GSE151352 GBM datasets from gene expression omnibus used in real data application. **b).** Venn diagram of the differentially expressed genes identified using inverse-normal (IN DEGs), modified inverse-normal (MIN DEGs) and fused inverse-normal (FIN DEGs) methods.

The remaining transcripts were then normalized using the TMM method [32]. Common and tag-wise dispersion were estimated and a negative-binomial generalized log-linear model was fitted to the read counts using the glmFit function under the edgeR package. Raw p-values were then obtained from the differential analysis for case/control conditions. More information about the DEGs identified in per-study differential analysis based on the criteria $|\log_2 FC| > 1$ and FDR p-value < 0.05 can be found in Table 2. We note that TCGA-GBM dataset has a much larger library size (~ 47 million reads, Illumina HiSeq 2000 v2 sequencer) as compared to GSE151352 (~ 4 million reads, Ion Torrent S5 sequencer) and GSE123892 (~ 35 million reads, Illumina HiSeq 2500 sequencer). Hence, we observed a differing number of genes left after filtering and consequently a much larger number of DEGs being observed for TCGA-GBM dataset as compared to the other two (Table 2) [33] in per-study differential expression analysis. As the sequencing output gets larger, the smaller count differences between samples are declared significant by models for differential expression in edgeR. A more detailed treatment of differential expression in RNA-seq data and how it is affected by sequencing depth and other factors can be found in Tarazona et al. (2011) [33].

Moreover, we also considered individual differential analysis for TCGA-GBM RNA-seq data by randomly selecting 20 cases together with available 5 normal samples in order to make all three datasets (GSE123892, GSE151352 and TCGA-GBM) comparable in terms of number of replicates for the meta-analysis (see Supplementary 1: Table 2). Hence, we considered two different meta-analysis scenarios.

Meta-analysis

Once the raw p-values were obtained from the individual differential expression analysis for each dataset, IN, MIN and FIN methods were then applied for p-value combination. Since the TCGA-GBM dataset (160 GBM vs 5 normal samples) is much larger in terms of number of samples as compared to GSE123892 (4 GBM vs 3 normal samples) and GSE151352 (12 GBM vs 12 normal samples), we considered two different combination scenarios. First, all TCGA-GBM samples were used for individual analysis to obtain the raw p-values. Second, 20 cases and 5 normal samples randomly selected from TCGA-GBM dataset were considered for individual analysis to get raw p-values and then considered for meta-analysis with the other

two datasets (GSE123892 and GSE151352). 10 different random selections were made and individual differential expression analysis were conducted respectively. Second scenario ensured that the datasets included in meta-analysis had comparable sample sizes.

In scenario one, a total of 18325 unique gene pool was considered for meta-analysis which was the combination of genes identified in each RNA-seq data analysis after quality control and filtering (Table 2). 13056 out of 18325 genes (~71%) were found to have the same direction of expression across the studies in which they were present whereas 5259 (~29%) of genes had conflicting or mismatched direction of expression. The direction of expression for a gene in an individual study was determined based on the sign of $\log_2 FC$ obtained for that gene in per-study differential analysis. Hence, only 13056 genes were effectively considered for IN method as compared to 18325 genes for MIN and FIN methods for identifying DEGs because of post-hoc removal of DEGs with conflicting direction of expression in the IN method.

For each of the combination methods, we assessed the number of DEGs based on average absolute log fold-change $\sum_{i=1}^n |\log_2 FC_i|/n > 1$ and FDR p-value < 0.05 criteria. Here, n denotes the number of datasets in which a particular gene was present. In case a gene was absent in a dataset, the weights in the combination methods were estimated only using the number of replicates in datasets in which the gene was present. The three p-value combination methods were then compared based on number of DEGs identified and unique DEGs identified by each method. A total of 5918, 5892 and 6138 DEGs were identified by the IN, MIN and FIN methods respectively. Of the DEGs detected by all these meta-analysis methods, more than 90% of them were in common (Figure 4b) with FIN method having a higher detection power than the other two methods. Moreover, MIN and FIN method identified a total of 233 and 235 DEGs with mismatched direction of expression across studies by incorporating the direction of expression information. More importantly, in the subset of DEGs which were present in all three datasets, 5.26% of DEGs had conflicting direction of expression across studies. Although, small in proportion, this would be of importance in case a gene of interest for the disease being studied has conflicting direction of expression across different studies. Particularly when more datasets are included in meta-analysis, the number of genes considered in IN approach can be massively reduced.

Given that the FIN method has the highest power of DEG detection, we further explore the DEGs obtained using this meta-analysis procedure. Top 10 up and down-regulated DEGs identified by FIN method are presented in Table 3. For full list of DEGs identified by different meta-analysis methods, see Supplementary 2, 3 and 4. In terms of effective direction of expression of DEGs, 2914 DEGs with same direction of expression across studies and 180 DEGs with mismatched direction of expression were up-regulated. Similarly, 2989 (same direction) and 55 (mismatched direction) DEGs were down-regulated. Results for scenario 2 for random selection have been detailed in Supplementary 1: Table 3, 4 and 5.

DEGs (Up)	N_g	Mean logFC	Effect	BH p-value	DEGs (Down)	N_g	Mean logFC	Effect	BH p-value
<i>EIF4EBP1</i>	10.45	3.33	+++	$< 1.62 \times 10^{-15}$	<i>SMAD12</i>	11.19	4.32	---	$< 1.62 \times 10^{-15}$
<i>WEE1</i>	10.39	4.04	+++	$< 1.62 \times 10^{-15}$	<i>RASGRF2</i>	11.10	4.19	---	$< 1.62 \times 10^{-15}$
<i>VIM</i>	10.39	3.68	+++	$< 1.62 \times 10^{-15}$	<i>DNAJC6</i>	11.07	3.71	---	$< 1.62 \times 10^{-15}$
<i>NUSAP1</i>	10.29	4.67	+++	$< 1.62 \times 10^{-15}$	<i>SERPINI1</i>	10.99	4.79	---	$< 1.62 \times 10^{-15}$
<i>HJURP</i>	10.24	5.79	+++	$< 1.62 \times 10^{-15}$	<i>ATP1B1</i>	10.98	3.35	---	$< 1.62 \times 10^{-15}$
<i>KIF4A</i>	10.15	4.48	+++	$< 1.62 \times 10^{-15}$	<i>ATP8A1</i>	10.91	3.95	---	$< 1.62 \times 10^{-15}$
<i>KIF20A</i>	10.12	5.80	+++	$< 1.62 \times 10^{-15}$	<i>JAKMIP3</i>	10.91	4.40	---	$< 1.62 \times 10^{-15}$

<i>AURKB</i>	10.09	5.48	+++	$< 1.62 \times 10^{-15}$	<i>MFSD6</i>	10.90	2.83	---	$< 1.62 \times 10^{-15}$
<i>UBE2C</i>	10.07	5.95	+++	$< 1.62 \times 10^{-15}$	<i>DCTN1-ASI</i>	10.88	5.33	---	$< 1.62 \times 10^{-15}$
<i>CCNB2</i>	10.04	4.63	+++	$< 1.62 \times 10^{-15}$	<i>PRKACB</i>	10.85	2.35	---	$< 1.62 \times 10^{-15}$

Table 3. Top 10 up- and down-regulated DEGs identified by FIN method. The DEGs have been sorted based on the value of the statistic N_g and the mean of absolute value of the $\log_2 FC$ have been reported. Effect signifies the direction of expression of DEGs in the per-study differential analysis.

Pathway analysis and biological significance

DEGs obtained by the FIN method were further explored to assess their biological relevance to GBM. QIAGEN’s Ingenuity Pathway Analysis (IPA) (www.qiagen.com/ingenuity) tool was used to identify biological pathways in which DEGs were enriched and upstream regulator analysis (URA) identified upstream regulators for GBM. We performed pathway analysis and URA separately for DEGs that were up-regulated and down-regulated and were present in all three datasets. We also note that not all identified DEGs by the meta-analysis methods are present in all three studies considered. Number of DEGs present in one, two or all three datasets have been detailed in Table 4.

Method	Expression direction	Present in one study	Present in two studies	Present in three studies	Total DEGs
IN	Same	1368	1085	3465	5918
	Mismatched	0	0	0	
MIN	Same	1182	1035	3442	5892
	Mismatched	0	52	181	
FIN	Same	1359	1083	3461	6138
	Mismatched	0	53	182	

Table 4. Number of DEGs found in one, two or all three datasets. Same and mismatched represents if the direction of expression of a DEG was consistent across a study or not respectively.

Of 1798 up-regulated DEGs, all of them mapped in the IPA database and 128 canonical pathways were identified based on BH adjusted p-value (< 0.01). These include Hepatic Fibrosis Signaling Pathway (adj. Pval. = 3.98×10^{-13} , ratio = 0.205), Kinetochore Metaphase Signaling Pathway (adj. Pval. = 7.94×10^{-15} , ratio = 0.376), Cell Cycle Control of Chromosomal Replication (adj. Pval. = 5.89×10^{-09} , ratio = 0.393), Role of BRCA1 in DNA Damage Response (adj. Pval. = 1.32×10^{-08} , ratio = 0.325) and IL-8 Signaling (adj. Pval. = 4.37×10^{-08} , ratio = 0.215) as some of the top dysregulated pathways. More importantly, major aberrant pathways shown to be involved in GBM pathogenesis [34][35] were also identified and include Glioblastoma Multiforme Signaling (adj. Pval. = 2.95×10^{-06} , ratio = 0.206), Glioma Signaling (adj. Pval. = 3.63×10^{-05} , ratio = 0.205), p53 Signaling (adj. Pval. = 5.25×10^{-05} , ratio = 0.224), Glioma Invasiveness Signaling (adj. Pval. = 0.0008, ratio = 0.219), PI3K/AKT Signaling (adj. Pval. = 0.005, ratio = 0.146) and mTOR Signaling (adj. Pval. = 0.007, ratio = 0.138).

Similarly, all 1845 down-regulated DEGs mapped to the IPA database and 98 canonical pathways were identified as significant (BH adjusted p-value < 0.01). Synaptogenesis Signaling Pathway (adj. Pval. = 3.16×10^{-25} , ratio = 0.288), Endocannabinoid Neuronal Synapse Pathway (adj. Pval. = 1.00×10^{-16} , ratio = 0.359), Opioid Signaling Pathway (adj. Pval. = 1.00×10^{-13} , ratio = 0.247), GNRH Signaling (adj. Pval. = 6.31×10^{-11} , ratio = 0.260), Calcium Signaling (adj. Pval. = 6.31×10^{-11} , ratio = 0.243), G Beta Gamma

Signaling (adj. Pval. = 9.33×10^{-10} , ratio = 0.287) and Dopamine-DARPP32 Feedback in cAMP Signaling (adj. Pval. = 1.55×10^{-09} , ratio = 0.252) were identified as some of the top dysregulated pathways. The top 10 pathways identified by the up-regulated and down-regulated DEGs separately are illustrated in Figure 5. For complete list of identified pathways for up- and down-regulated DEGs in our study, see Supplementary 1: Table 6.

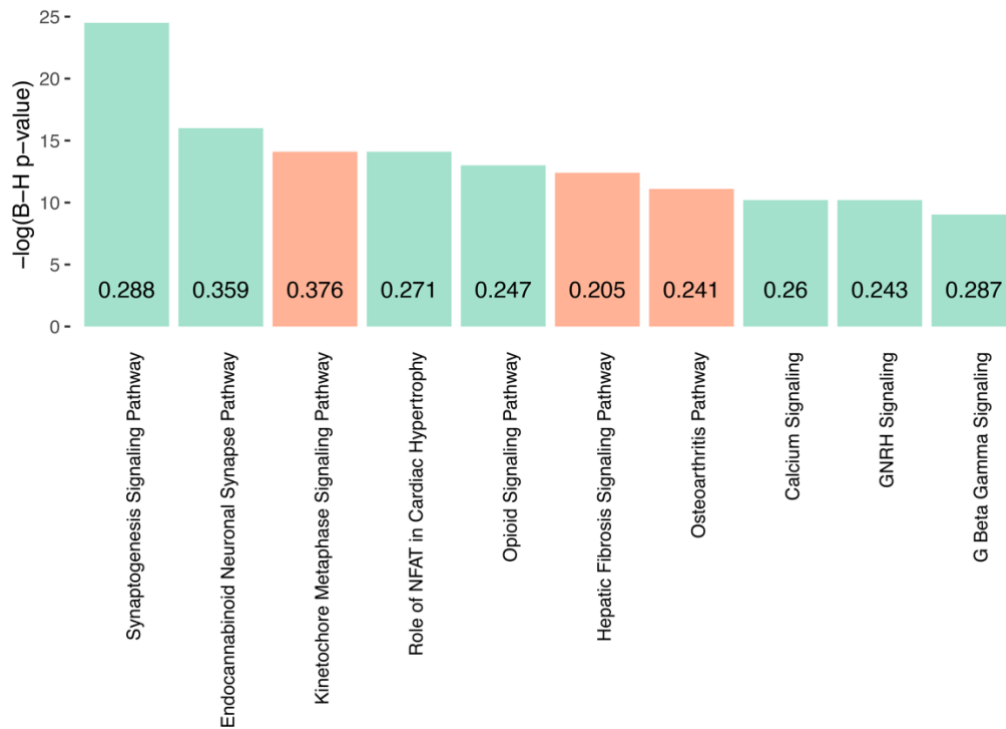


Figure 5. Significant pathways identified by IPA. The top ten significant pathways based on BH p-value among the canonical pathways identified by IPA for the up-regulated DEGs (orange bar) and down-regulated DEGs (green bar). The numbers on the bar plot show the ratio between the numbers of DEGs enriched and total number of genes in each of these pathways.

In addition, the URA tool in IPA identified potential upstream regulators (transcription factors, genes or other small molecules) that has been experimentally observed to affect gene expression. It identifies these regulators by analysing linkage to DEGs through coordinated expression [36]. Among the up-regulated DEGs, *TGFB1* and *TP53*, which are also DEGs and important in GBM pathogenesis [37][38] are predicted to be the top two upstream regulators. 293 up-regulated DEGs were identified as potential upstream regulators of gene upregulation out of a total of 2215 (BH corrected p-value < 0.01, see Supplementary 1: Table 7a) predicted upstream regulators. Out of 2215 predicted, 764 of these significant upstream regulators were activated and 112 were also observed as DEGs in our analysis.

On the contrary, for the down-regulated DEGs, IPA identified 32 potential upstream regulators (BH corrected p-value < 0.01, see Supplementary 1: Table 7b) with *TCF7L2* and *MAPT* as the top two. 14 of the 32 upstream regulated were predicted to be inhibited and two among the inhibited are DEGs. *TCF7L2* is a diabetes risk-associated gene which plays a key role in the Wnt-signaling pathway and is shown to be frequently mutated in colorectal cancer [39] and promote cell proliferation [40]. However, exploration of its role in GBM pathogenesis warrant further studies. Interestingly, *MAPT* is also a DEG observed in our analysis and is one of the two hallmarks of AD [41]. Gargini et al. (2019) [42] observed a strong correlation of

Tau/MAPT expression and indicators of survival in glioma patients. Moreover, it has been found to be epigenetically controlled by balance between *IDH1/2* wild-type and mutation in human gliomas [43]. Thus, providing further evidence and reaffirming the involvement of *MAPT* in central nervous system disorders.

Of the DEGs with conflicting direction of expression across studies, 182 out of 235 DEGs are present in all three datasets. Among them *CMTM6*, *RAD51*, *NOS1AP*, *MSANTD1*, *PGM2*, *PSD3*, *GPR82*, *SPTBN4*, *TSPAN6* and *ARHGEF28* were identified as top 10 DEGs based on the absolute value of N_g (see Table 5). Interestingly, *RAD51* and *ARHGEF28* have previously been identified as a tumour suppressor and an oncogene respectively [44]. More importantly, *RAD51* was found to be effectively overexpressed in GBM in our study and have recently been shown as a target for inhibition to enhance radiosensitivity of GBM cells during treatment [45][46]. On the other hand, *ARHGEF28* was found to be effectively down-regulated in our study. It is an intracellular kinase that functions either as a Rho guanine exchange factor or a scaffolding protein to initiate FAK activation and cell contractibility [47]. Furthermore, the RhoA-FAK pathway has been shown to be involved in colon cancer cell proliferation and migration [48]. *ARHGEF28* mRNA levels have also been found to be elevated in late-stage ovarian cancer and associated with decreased progression free and overall survival [49]. However, its role in GBM growth and progression is yet to be elucidated and requires exploration in future studies.

DEGs	N_g	Mean $ \log_{2}FC $	Effect	BH p-value
<i>CMTM6</i>	7.58	1.30	+++	3.93×10^{-13}
<i>RAD51</i>	7.58	2.82	+++	4.03×10^{-13}
<i>NOS1AP</i>	-7.53	1.37	+-	5.73×10^{-13}
<i>MSANTD1</i>	-7.53	1.31	+-	5.92×10^{-13}
<i>PGM2</i>	7.52	1.31	+++	6.35×10^{-13}
<i>PSD3</i>	-7.47	1.67	+-	8.63×10^{-13}
<i>GPR82</i>	7.43	4.35	+++	1.24×10^{-12}
<i>SPTBN4</i>	-7.31	1.91	+-	2.78×10^{-12}
<i>TSPAN6</i>	7.18	2.08	+++	6.86×10^{-12}
<i>ARHGEF28</i>	-7.06	1.23	+-	1.63×10^{-11}

Table 5. Top 10 DEGs with mismatched direction of expression across datasets identified by FIN method. The DEGs have been sorted based on the absolute value of the statistic N_g and the mean of absolute value of the $\log_2 FC$ have been reported. Effect signifies the direction of expression of DEGs in the per-study differential analysis for GSE123892, GSE151352 and TCGA-GBM respectively.

Discussion

Although the implementation of MIN and FIN p-value combination methods are straight forward, they require some additional considerations. First, the used weighting criteria leads to a larger weight being given to a study with larger sample sizes. Intuitively, this is expected as a study with a larger sample size might be more robust than studies with lower sample sizes. However, importance must also be given to the quality of the RNA-seq data in each study. It must be assessed in case this information is available and other weights more appropriate as per the quality of the data may be specified. In our study, since TCGA-GBM has a much larger sample size as compared to the other two datasets, we compared the number of DEGs obtained by FIN method by considering all 165 samples and 10 random selections of 20 cases and 5 normal samples. On average, about 94% of the DEGs obtained when randomly selected subset was considered were also found in DEGs identified using the full TCGA-GBM dataset (see

Supplementary 1: Table 8). Hence, suggesting that the identification of DEGs was stable across these two settings.

Next, the MIN and FIN are adaptive in a sense that they allow for consideration of genes that may not be present in all studies that are considered for integrated differential expression analysis. In case a gene is not present in some of the studies, the weights (w_s) in the combination method can only be estimated using the number of replicates in the datasets in which the gene is present. However, for genes that are just present in one study, it would mean that the results from the meta-analysis for these genes would be the same as the per-study differential analysis. Hence, a careful consideration about the quality of the RNA-seq data and library size is required in case only the genes that are common among studies are considered. For datasets of similar quality and library size, a large proportion of genes would not be excluded from meta-analysis if only common genes are used. However, a large number of genes might be excluded from meta-analysis in case of dissimilar library sizes and quality which could lead to potentially missing out on important genes for the disease. For instance, only 12345 out of 18315 unique genes are present in all 3 studies in our application where the library sizes are not similar. Thus, a balanced approach is suggested.

Finally, we used edgeR for per-study differential analysis in our study but other popular packages such as DESeq2 [50] and NOIseq [33] can be applied. Moreover, the FIN model can be extended to multi-group comparisons apart from a two-group comparison discussed in this study. The proposed meta-analysis method relies on the fact that the same test statistics are used for per-study differential expression analysis to obtain individual p-values and all studies under consideration have the same experimental considerations. For instance, in case DESeq2 is used for multi-group differential expression analysis in each study, a likelihood ratio test is used rather than Wald statistics being used for two group differential expression analysis.

Conclusions

In this study, we proposed MIN and consequently FIN method for meta-analysis of RNA-seq data. The developed methods account for both the sample size of study and direction of expression of a gene in each study allowing for detection of potentially robust biologically significant DEGs even when they have conflicting direction of expression across studies. In contrast with the existing IN method, the proposed methods have the advantage of identifying DEGs among genes with conflicting direction of expression across studies. For the genes with concordant differential expression patterns across studies the MIN method exhibited a similar DEG detection power and performance as compared to IN method particularly when there was high inter-study variability and increased number of studies were considered. FIN method exhibited a similar or improved DEG detection power as compared to IN method and was significantly better in performance as compared to MIN method. More importantly, in a real data application, we demonstrated the use of FIN method in detection of biologically relevant DEGs to GBM. Hence, this meta-analysis method provides a way to establish differential expression status for genes with conflicting direction of expression in individual RNA-seq studies and further exploration of them as potential biomarkers for the disease. With lowering costs and increase in the number of RNA-seq studies being archived on public databases, this method might provide a way to integrate a greater number of studies without losing much prior information and consequently considering all the genes in the analysis irrespective of their direction of expression.

Declarations

Ethics approval and consent to participate

Not applicable

Consent for publication

Not applicable

Availability of data and materials

All datasets used in study are publicly accessible and appropriate access links have been provided in the text of the manuscript when they have been first mentioned. An implementation of the proposed method can be found here:

https://github.com/nash5202/FIN_meta_analysis/

Competing interests

The authors declare that they have no competing interests.

Funding

This research was supported by AiPBAND (www.aipband-itn.eu), European Union's Horizon 2020 research and innovation programme under the Marie Skłodowska-Curie grant agreement 764281. BP is a Marie-Curie early-stage research fellow of AiPBAND.

Authors' contributions

BP and XL conceived and designed the study. BP performed simulations, data analysis and interpretation and drafted the manuscript. XL helped interpret the results, reviewed and edited the manuscript. All authors read and approved the final manuscript.

Authors' information

¹National Horizons Centre, School of Health and Life Sciences, Teesside University, Darlington, DL1 1HG, UK.

*Correspondence: Email: X.Li@tees.ac.uk, Phone: [+44-01642738451](tel:+44-01642738451)

References

1. Marioni JC, Mason CE, Mane SM, Stephens M, Gilad Y. RNA-seq: an assessment of technical reproducibility and comparison with gene expression arrays. *Genome research*. 2008 Sep 1;18(9):1509-17.
2. Cancer Genome Atlas Research Network. Comprehensive genomic characterization defines human glioblastoma genes and core pathways. *Nature*. 2008 Oct;455(7216):1061.
3. Sanchez-Vega F, Mina M, Armenia J, Chatila WK, Luna A, La KC, Dimitriadoy S, Liu DL, Kantheti HS, Saghafinia S, Chakravarty D. Oncogenic signaling pathways in the cancer genome atlas. *Cell*. 2018 Apr 5;173(2):321-37.
4. Weinstein JN, Collisson EA, Mills GB, Shaw KR, Ozenberger BA, Ellrott K, Shmulevich I, Sander C, Stuart JM, Cancer Genome Atlas Research Network. The cancer genome atlas pan-cancer analysis project. *Nature genetics*. 2013 Sep 26;45(10):1113.
5. Zhao Z, Meng F, Wang W, Wang Z, Zhang C, Jiang T. Comprehensive RNA-seq transcriptomic profiling in the malignant progression of gliomas. *Scientific data*. 2017 Mar 14;4(1):1-7.
6. Wan YW, Al-Ouran R, Mangleburg CG, Perumal TM, Lee TV, Allison K, Swarup V, Funk CC, Gaiteri C, Allen M, Wang M. Meta-analysis of the Alzheimer's disease human brain transcriptome and functional dissection in mouse models. *Cell reports*. 2020 Jul 14;32(2):107908.
7. Tseng GC, Ghosh D, Feingold E. Comprehensive literature review and statistical considerations for microarray meta-analysis. *Nucleic acids research*. 2012 May 1;40(9):3785-99.

8. Hong F, Breitling R. A comparison of meta-analysis methods for detecting differentially expressed genes in microarray experiments. *Bioinformatics*. 2008 Feb 1;24(3):374-82.
9. Hu P, Greenwood CM, Beyene J. Statistical methods for meta-analysis of microarray data: a comparative study. *Information Systems Frontiers*. 2006 Feb 1;8(1):9-20.
10. Rau A, Marot G, Jaffrézic F. Differential meta-analysis of RNA-seq data from multiple studies. *BMC bioinformatics*. 2014 Dec 1;15(1):91.
11. Toro-Domínguez D, Villatoro-García JA, Martorell-Marugán J, Román-Montoya Y, Alarcón-Riquelme ME, Carmona-Sáez P. A survey of gene expression meta-analysis: methods and applications. *Briefings in Bioinformatics*. 2020 Feb 25.
12. Choi JK, Yu U, Kim S, Yoo OJ. Combining multiple microarray studies and modeling interstudy variation. *Bioinformatics*. 2003 Jul 3;19(suppl_1):i84-90.
13. Marot G, Foulley JL, Mayer CD, Jaffrézic F. Moderated effect size and P-value combinations for microarray meta-analyses. *Bioinformatics*. 2009 Oct 15;25(20):2692-9.
14. Breitling R, Armengaud P, Amtmann A, Herzyk P. Rank products: a simple, yet powerful, new method to detect differentially regulated genes in replicated microarray experiments. *FEBS letters*. 2004 Aug 27;573(1-3):83-92.
15. Sonesson C, Delorenzi M. A comparison of methods for differential expression analysis of RNA-seq data. *BMC bioinformatics*. 2013 Dec 1;14(1):91.
16. Oshlack A, Robinson MD, Young MD. From RNA-seq reads to differential expression results. *Genome biology*. 2010 Dec 1;11(12):220.
17. Kulinskaya E, Morgenthaler S, Staudte RG. *Meta analysis: a guide to calibrating and combining statistical evidence*. John Wiley & Sons; 2008 Apr 15.
18. Moulos P, Hatzis P. Systematic integration of RNA-Seq statistical algorithms for accurate detection of differential gene expression patterns. *Nucleic acids research*. 2015 Feb 27;43(4):e25-.
19. Tsuyuzaki K, Nikaido I. metaSeq: Meta-analysis of RNA-Seq count data in multiple studies. *R Package*. version. 2013;1(0).
20. Li X, Long J, He T, Belshaw R, Scott J. Integrated genomic approaches identify major pathways and upstream regulators in late onset Alzheimer's disease. *Scientific reports*. 2015 Jul 23;5:12393.
21. Ma T, Liang F, Tseng G. Biomarker detection and categorization in ribonucleic acid sequencing meta-analysis using bayesian hierarchical models. *Journal of the Royal Statistical Society. Series C, Applied statistics*. 2017 Aug;66(4):847.
22. Huo Z, Tang S, Park Y, Tseng G. P-value evaluation, variability index and biomarker categorization for adaptively weighted Fisher's meta-analysis method in omics applications. *Bioinformatics*. 2020 Jan 15;36(2):524-32.
23. Huo Z, Song C, Tseng G. Bayesian latent hierarchical model for transcriptomic meta-analysis to detect biomarkers with clustered meta-patterns of differential expression signals. *The annals of applied statistics*. 2019 Mar;13(1):340.
24. Robinson MD, McCarthy DJ, Smyth GK. edgeR: a Bioconductor package for differential expression analysis of digital gene expression data. *Bioinformatics*. 2010 Jan 1;26(1):139-40.
25. Marot G, Mayer CD. Sequential analysis for microarray data based on sensitivity and meta-analysis. *Statistical Applications in Genetics and Molecular Biology*. 2009 Jan 21;8(1).
26. Benjamini Y, Hochberg Y. Controlling the false discovery rate: a practical and powerful approach to multiple testing. *Journal of the Royal statistical society: series B (Methodological)*. 1995 Jan;57(1):289-300.

27. Barrett T, Wilhite SE, Ledoux P, Evangelista C, Kim IF, Tomashevsky M, Marshall KA, Phillippy KH, Sherman PM, Holko M, Yefanov A. NCBI GEO: archive for functional genomics data sets—update. *Nucleic acids research*. 2012 Nov 26;41(D1):D991-5.
28. Enis Afgan, Dannon Baker, B er enice Batut, Marius van den Beek, Dave Bouvier, Martin ech, John Chilton, Dave Clements, Nate Coraor, Bj orn Gr uning, Aysam Guerler, Jennifer Hillman-Jackson, Vahid Jalili, Helena Rasche, Nicola Soranzo, Jeremy Goecks, James Taylor, Anton Nekrutenko, and Daniel Blankenberg. The Galaxy platform for accessible, reproducible and collaborative biomedical analyses: 2018 update, *Nucleic Acids Research*, Volume 46, Issue W1, 2 July 2018, Pages W537–W544, doi:10.1093/nar/gky379
29. Martin M. Cutadapt removes adapter sequences from high-throughput sequencing reads. *EMBnet. journal*. 2011 May 2;17(1):10-2.
30. Dobin A, Davis CA, Schlesinger F, Drenkow J, Zaleski C, Jha S, Batut P, Chaisson M, Gingeras TR. STAR: ultrafast universal RNA-seq aligner. *Bioinformatics*. 2013 Jan 1;29(1):15-21.
31. Carlson M. org. Hs. eg. db: Genome Wide Annotation for Human. R package version 3.8. 2.
32. Robinson MD, Oshlack A. A scaling normalization method for differential expression analysis of RNA-seq data. *Genome biology*. 2010 Mar;11(3):1-9.
33. Tarazona S, Garc a-Alcalde F, Dopazo J, Ferrer A, Conesa A. Differential expression in RNA-seq: a matter of depth. *Genome research*. 2011 Dec 1;21(12):2213-23.
34. Pearson JR, Regad T. Targeting cellular pathways in glioblastoma multiforme. *Signal transduction and targeted therapy*. 2017 Sep 29;2(1):1-1.
35. Mao H, LeBrun DG, Yang J, Zhu VF, Li M. Deregulated signaling pathways in glioblastoma multiforme: molecular mechanisms and therapeutic targets. *Cancer investigation*. 2012 Jan 1;30(1):48-56.
36. Kramer A, Green J, Pollard Jr J, Tugendreich S. Causal analysis approaches in Ingenuity Pathway Analysis. *Bioinformatics*. 2014;30(4):523-30.
37. Frei K, Gramatzki D, Tritschler I, Schroeder JJ, Espinoza L, Rushing EJ, Weller M. Transforming growth factor- pathway activity in glioblastoma. *Oncotarget*. 2015 Mar 20;6(8):5963.
38. Suh SS, Yoo JY, Nuovo GJ, Jeon YJ, Kim S, Lee TJ, Kim T, Bakacs A, Alder H, Kaur B, Aqeilan RI. MicroRNAs/TP53 feedback circuitry in glioblastoma multiforme. *Proceedings of the National Academy of Sciences*. 2012 Apr 3;109(14):5316-21.
39. Cancer Genome Atlas Network. Comprehensive molecular characterization of human colon and rectal cancer. *Nature*. 2012 Jul;487(7407):330.
40. Bass AJ, Lawrence MS, Brace LE, Ramos AH, Drier Y, Cibulskis K, Sougnez C, Voet D, Saksena G, Sivachenko A, Jing R. Genomic sequencing of colorectal adenocarcinomas identifies a recurrent VTI1A-TCF7L2 fusion. *Nature genetics*. 2011 Oct;43(10):964-8.
41. Long JM, Holtzman DM. Alzheimer disease: an update on pathobiology and treatment strategies. *Cell*. 2019 Oct 3;179(2):312-39.
42. Gargini R, Segura-Collar B, S anchez-G omez P. Novel functions of the neurodegenerative-related gene tau in cancer. *Frontiers in aging neuroscience*. 2019;11:231.
43. Gargini R, Segura-Collar B, Herr anz B, Garc a-Escudero V, Romero-Bravo A, N unez FJ, Garc a-P erez D, Guti errez-Guam an J, Ayuso-Sacido A, Seoane J, P erez-N unez A. The IDH-TAU-EGFR triad defines the neovascular landscape of diffuse gliomas. *Science Translational Medicine*. 2020 Jan 22;12(527).

44. Chakravarty D, Gao J, Phillips S, Kundra R, Zhang H, Wang J, Rudolph JE, Yaeger R, Soumerai T, Nissan MH, Chang MT. OncoKB: a precision oncology knowledge base. *JCO precision oncology*. 2017 May;1:1-6.
45. Navarra G, Pagano C, Pacelli R, Crescenzi E, Longobardi E, Gazzero P, Fiore D, Pastorino O, Pentimalli F, Laezza C, Bifulco M. N6-Isopentenyladenosine enhances the radiosensitivity of glioblastoma cells by inhibiting the homologous recombination repair protein RAD51 expression. *Frontiers in oncology*. 2020 Jan 14;9:1498.
46. Ma J, Benitez JA, Li J, Miki S, de Albuquerque CP, Galatro T, Orellana L, Zanca C, Reed R, Boyer A, Koga T. Inhibition of nuclear PTEN tyrosine phosphorylation enhances glioma radiation sensitivity through attenuated DNA repair. *Cancer cell*. 2019 Mar 18;35(3):504-18.
47. Miller NL, Lawson C, Kleinschmidt EG, Tancioni I, Uryu S, Schlaepfer DD. A non-canonical role for Rgnef in promoting integrin-stimulated focal adhesion kinase activation. *Journal of cell science*. 2013 Nov 1;126(21):5074-85.
48. Yu HG, Nam JO, Miller NL, Tanjoni I, Walsh C, Shi L, Kim L, Chen XL, Tomar A, Lim ST, Schlaepfer DD. p190RhoGEF (Rgnef) promotes colon carcinoma tumor progression via interaction with focal adhesion kinase. *Cancer research*. 2011 Jan 15;71(2):360-70.
49. Kleinschmidt EG, Miller NL, Ozmadenci D, Tancioni I, Osterman CD, Barrie AM, Taylor KN, Ye A, Jiang S, Connolly DC, Stupack DG. Rgnef promotes ovarian tumor progression and confers protection from oxidative stress. *Oncogene*. 2019 Sep;38(36):6323-37.
50. Love MI, Huber W, Anders S. Moderated estimation of fold change and dispersion for RNA-seq data with DESeq2. *Genome biology*. 2014 Dec 1;15(12):550.

Figures, tables and additional files

Figures

Figure 3. Performance comparison of modified inverse-normal, inverse-normal and fused inverse-normal methods. Plots of receiver operating characteristics (ROC) curves averaged over 100 trials for each simulation setting. Simulation settings are represented by rows (from top to bottom): corresponding to low ($\sigma = 0.15$) and high ($\sigma = 0.5$) inter-study variability and columns (from left to right): corresponding to 3 ($S=3$) and 5 studies ($S=5$) combined. The red, turquoise and magenta ROC curves represent the modified inverse-normal, inverse-normal and fused inverse-normal methods respectively.

Figure 4. Characteristics of modified inverse-normal method. a). False discovery rates for modified inverse-normal method for all simulation settings. **b).** Proportion of true-positives (TPs) among unique differentially expressed genes (DEGs) identified by modified inverse-normal (MIN) method as compared to inverse-normal (IN) method. **c).** Proportion of unique DEGs (MIN) with the observed effective direction of expression as the true direction of expression.

Figure 3. Characteristics of fused inverse-normal method. a). False discovery rates for fused inverse-normal method for all simulation settings. **b).** Proportion of true-positives (TPs) among unique differentially expressed genes (DEGs) identified by fused inverse-normal (FIN) method as compared to inverse-normal (IN) method. **c).** Proportion of unique DEGs (FIN) with the observed effective direction of expression as the true direction of expression.

Figure 4. Comparison of results from meta-analysis methods. a). Histograms of raw p-values obtained from per-study differential analysis of GSE123892 and GSE151352 GBM

datasets from gene expression omnibus used in real data application. **b).** Venn diagram of the differentially expressed genes identified using inverse-normal (IN DEGs), modified inverse-normal (MIN DEGs) and fused inverse-normal (FIN DEGs) methods.

Figure 5. Significant pathways identified by IPA. The top ten significant pathways based on BH p-value among the canonical pathways identified by IPA for the up-regulated DEGs (orange bar) and down-regulated DEGs (green bar). The numbers on the bar plot show the ratio between the numbers of DEGs enriched and total number of genes in each of these pathways.

Tables

Table 1. Simulation settings for inter-study variability parameter (σ), number of studies and number of replicates per study. Area under the ROC curves (AUC) for IN, MIN and FIN methods computed using 100 trials for each simulation setting.

Table 2. Information about GBM RNA-seq datasets used for integrated analysis using different p-value combination methods in our study. Up and down DEGs refer to the up and down-regulated DEGs obtained in per-study differential analysis.

Table 3. Top 10 up- and down-regulated DEGs identified by FIN method. The DEGs have been sorted based on the value of the statistic N_g and the mean of absolute value of the $\log_2 FC$ have been reported. Effect signifies the direction of expression of DEGs in the per-study differential analysis.

Table 4. Number of DEGs found in one, two or all three datasets. Same and mismatched represents if the direction of expression of a DEG was consistent across a study or not respectively.

Table 5. Top 10 DEGs with mismatched direction of expression across datasets identified by FIN method. The DEGs have been sorted based on the absolute value of the statistic N_g and the mean of absolute value of the $\log_2 FC$ have been reported. Effect signifies the direction of expression of DEGs in the per-study differential analysis for GSE123892, GSE151352 and TCGA-GBM respectively.

Supplementary Information

Supplementary 1. Document contains interpretation of the FIN model, details of RNA-seq raw data processing using GALAXY, brief description of the simulation method, results of scenario 2 considered for meta-analysis and Ingenuity pathway analysis results.

Supplementary 2. Full list of DEGs identified in scenario 1 by the inverse-normal method in GBM data application.

Supplementary 3. Full list of DEGs identified in scenario 1 by the modified inverse-normal method in GBM data application.

Supplementary 4. Full list of DEGs identified in scenario 1 by the fused inverse-normal method in GBM data application.

Fused inverse-normal method for integrated differential expression analysis of RNA-seq data

Birbal Prasad¹ and Xinzhong Li^{1*}

¹National Horizons Centre, School of Health and Life Sciences, Teesside University,

Darlington, DL1 1HG, UK. Email: B.Prasad@tees.ac.uk; X.Li@tees.ac.uk

*Correspondence: Email: X.Li@tees.ac.uk, Phone: [+44-01642738451](tel:+44-01642738451)

Supplementary information contents lists:

- 1. Interpretations of the FIN model**
- 2. Simulation study model**
- 3. Processing of raw RNA-seq dataset GSE151352 using GALAXY**
- 4. Supplementary Figure 1.** Flow of different steps used in processing of the raw RNA-seq fastq files for GSE151352 using Galaxy to get raw counts.
- 5. Supplementary Table 1.** Total number of genes (# genes), number of genes with conflicting direction of expression (# conf. genes), number of differentially expressed genes (# DEGs), number of genes with conflicting direction of expression (# conf. DEGs) and number of true DEGs (# true DEGs) for all simulation settings averaged over 100 trials.
- 6. Supplementary Table 2.** Total number of up and down-regulated DEGs identified in per-study differential analysis in 10 random selections of 20 GBM cases and 5 controls from TCGA-GBM dataset.
- 7. Supplementary Table 3.** Number of DEGs identified by the inverse-normal (IN) method in the GBM data application for both scenarios and number of these DEGs present in one, two or all three datasets considered.
- 8. Supplementary Table 4.** Number of DEGs identified by the modified inverse-normal (MIN) method in the GBM data application for both scenarios and number of these DEGs present in one, two or all three datasets considered.
- 9. Supplementary Table 5.** Number of DEGs identified by the fused inverse-normal (FIN) method in the GBM data application for both scenarios and number of these DEGs present in one, two or all three datasets considered.

- 10. Supplementary Table 6.** IPA canonical pathways for up and down-regulated DEGs present in all three GBM datasets and identified by the FIN method.
- 11. Supplementary Table 7.** IPA upstream regulator analysis results for up and down-regulated DEGs present in all three GBM datasets and identified by the FIN method.
- 12. Supplementary Table 8.** Number of common DEGs identified by the FIN method in both scenarios considered for TCGA-GBM data. On average about 94% of the DEGs obtained when randomly selected subset was considered were also found in DEGs identified using the full TCGA-GBM dataset.
- 13. Supplementary 2.** Full list of DEGs identified in scenario 1 by the inverse-normal method in GBM data application (in an Excel file).
- 14. Supplementary 3.** Full list of DEGs identified in scenario 1 by the modified inverse-normal method in GBM data application (in an Excel file).
- 15. Supplementary 4.** Full list of DEGs identified in scenario 1 by the fused inverse-normal method in GBM data application (in an Excel file).

Interpretations of the FIN model

In order to understand the practical behaviour and interpretations of the FIN model in different scenarios, we consider the following cases in terms of differential expression of a gene and its direction of expression (up: +, down: -) in individual studies:

- i. A gene is non differentially expressed (NDE) in one study and differentially expressed (DE) in another: If it is NDE, $\Phi^{-1}(1 - p_{gs})$ is standard normal distributed. Hence, it takes values around 0 with high probability. On the contrary, if it is DE, $\Phi^{-1}(1 - p_{gs})$ will take extreme values. Now, the value of N_g will then depend on which study has the larger weight (w_s).
- ii. A gene is strongly +DE in one study and strongly -DE in another: In this case, $\Phi^{-1}(1 - p_{gs})$ will be extreme for both studies. Then, if the weight w_s is similar for both studies, the contribution of the study specific term to N_g will cancel each other out because of B_{gs} . Hence, N_g which will be close to 0 will give us non-significant p-value in hypothesis testing for that gene. This makes sense as we will have comparable evidence of conflicting direction of expression for the gene. In case, the weight of one study is comparatively larger than the other study, we will get that the gene is DE with the effective sign of regulation of that of the bigger study.
- iii. A gene is strongly +DE in most studies and weakly -DE in a few: Similar to case ii, $\Phi^{-1}(1 - p_{gs})$ will be extreme for all the studies. For comparable weights of studies, we would get a large positive value for N_g as we have many more studies where the gene is +DE as compared to where the gene is -DE. Hence, resulting in the gene to be +DE after hypothesis testing. Only in case when the study where the gene is -DE has an extremely larger weight w_s as

compared to all other four studies combined can that gene be -DE as a result of the hypothesis testing.

Simulation study model

Here, we briefly describe the theoretical framework of the simulation study method adapted from Rau et al. (2014) [reference 10 in the manuscript]. For detailed procedure for estimation of parameter values based on real RNA-seq datasets (GSE125583 in this study), see Rau et al. (2014).

Let Y_{gcrs} be random variable with y_{gcrs} as its realisations which are observed count for a gene g , condition c , biological replicate r and study s . RNA-seq data was generated as per the negative binomial distribution,

$$Y_{gcrs} \sim NB(\mu_{gcs}, \phi_{gs})$$

where parameters μ_{gcs} and ϕ_{gs} represent the mean and dispersion, respectively, for a gene g , condition c and study s . To account for variability between the individual studies (inter-study variability) considered for meta-analysis, we consider the following situation:

$$\mu_{gcs} = \theta_{gc} \times e^{\epsilon_{gcs}}$$

where $\epsilon_{gcs} \sim N(0, \sigma^2)$. θ_{gc} is the mean for a gene g in condition c . ϵ_{gcs} represents the variability around θ_{gc} due to a study and condition specific random effect. σ^2 represents the size of the inter-study variability which affects μ_{gcs} through ϵ_{gcs} with ϵ_{gcs} having a multiplicative effect on μ_{gcs} .

Processing of raw RNA-seq dataset GSE151352 using GALAXY

Raw fastq files generated by GPL23934 (Ion Torrent S5 (Homo sapiens)) platform were retrieved for all 24 samples (12 tumour and 12 healthy) from Sequence Read Archive (<https://trace.ncbi.nlm.nih.gov/Traces/sra/sra.cgi?study=SRP265074>) using Get Data tool in Galaxy. Next, we assessed the quality of the raw reads using quality reports from FastQC and removed the specified adapter sequence ATCACCGACTGCCCATAGAGAGGCTGAGAC with Cutadapt (version 1.16). The parameters used for this step were the parameters provided by the submitted of the dataset on Gene Expression Omnibus. The adapter trimmed reads were again assessed for quality by FastQC and were aligned to the reference genome (GRCh37.p13, genecode v19) using a 2-pass method with RNA STAR (Galaxy version 2.7.5b) where other parameters used were default parameters. Following alignment, the generated BAM files were processed using the featureCounts tool (Galaxy version 1.6.4+galaxy2) to get raw counts for each RNA-seq data sample.

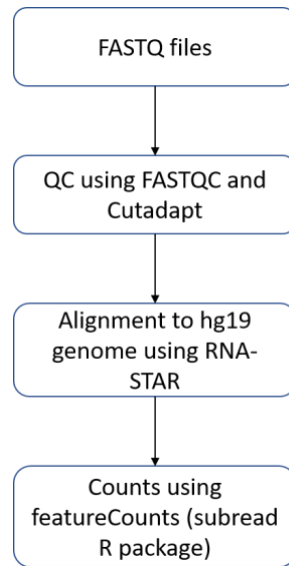


Figure 1. Flow of different steps used in processing of the raw RNA-seq fastq files for GSE151352 using Galaxy to get raw counts.

Supplementary Table 1. Total number of genes (# genes), number of genes with conflicting direction of expression (# conf. genes), number of differentially expressed genes (# DEGs), number of genes with conflicting direction of expression (# conf. DEGs) and number of true DEGs (# true DEGs) present for all simulation settings averaged over 100 trials.

Setting (σ , #studies)	# genes (IN/MIN/FIN)	# conf. genes (IN/MIN/FIN)	# DEGs (IN, MIN, FIN)	# conf. DEGs (IN, MIN, FIN)	# true DEGs
0.15, 3	16776 \pm 19	10099 \pm 49	2268 \pm 38, 2611 \pm 49, 2441 \pm 45	0, 243 \pm 18, 236 \pm 18	6436 \pm 10
0.15, 5	16871 \pm 17	13036 \pm 43	2431 \pm 35, 4031 \pm 47, 3741 \pm 45	0, 1365 \pm 39, 1337 \pm 38	6468 \pm 9
0.5, 3	17002 \pm 45	11490 \pm 57	2098 \pm 35, 3879 \pm 46, 3741 \pm 44	0, 1706 \pm 35, 1697 \pm 35	6501 \pm 19
0.5, 5	17266 \pm 34	14824 \pm 48	1124 \pm 31, 4453 \pm 48, 4365 \pm 46	0, 3264 \pm 46, 3257 \pm 45	6585 \pm 15

Supplementary Table 2. Total number of up and down-regulated DEGs identified in per-study differential analysis in 10 random selections of 20 GBM cases and 5 controls from TCGA-GBM dataset.

TCGA-GBM	DEGs (Up)	DEGs (Down)	Total
Selection 1	3112	3016	6128
Selection 2	3323	3013	6336
Selection 3	3204	3030	6234
Selection 4	3285	3054	6339
Selection 5	3267	3077	6344
Selection 6	3249	3069	6318
Selection 7	3293	2968	6261
Selection 8	3792	2885	6677
Selection 9	3311	3025	6336
Selection 10	3229	3088	6317

Supplementary Table 3. Number of DEGs identified by the inverse-normal (IN) method in the GBM data application for both scenarios and number of these DEGs present in one, two or all three datasets considered.

Datasets	DEGs Present in 1	DEGs Present in 2	DEGs Present in 3
GSE123892, GSE151352, TCGA-GBM (all samples)	1368	1085	3465
GSE123892, GSE151352, TCGA-GBM (random selection 1)	921	1082	3511
GSE123892, GSE151352, TCGA-GBM (random selection 2)	943	1080	3477
GSE123892, GSE151352, TCGA-GBM (random selection 3)	939	1079	3462
GSE123892, GSE151352, TCGA-GBM (random selection 4)	965	1080	3482
GSE123892, GSE151352, TCGA-GBM (random selection 5)	939	1076	3540
GSE123892, GSE151352, TCGA-GBM (random selection 6)	940	1100	3543
GSE123892, GSE151352, TCGA-GBM (random selection 7)	972	1055	3461
GSE123892, GSE151352, TCGA-GBM (random selection 8)	989	1106	3513
GSE123892, GSE151352, TCGA-GBM (random selection 9)	921	1083	3529
GSE123892, GSE151352, TCGA-GBM (random selection 10)	995	1080	3442

Supplementary Table 4. Number of DEGs identified by the modified inverse-normal (MIN) method in the GBM data application for both scenarios and number of these DEGs present in one, two or all three datasets considered. **a.** For DEGs with the same direction of expression across all three studies. **b.** For DEGs with conflicting direction of expression across studies.

a. For DEGs with the same direction of expression across all 3 studies			
Datasets	DEGs Present in 1	DEGs Present in 2	DEGs Present in 3
GSE123892, GSE151352, TCGA-GBM (all samples)	1182	1087	3623
GSE123892, GSE151352, TCGA-GBM (random selection 1)	832	1081	3658
GSE123892, GSE151352, TCGA-GBM (random selection 2)	844	1099	3662
GSE123892, GSE151352, TCGA-GBM (random selection 3)	861	1089	3616

GSE123892, GSE151352, TCGA-GBM (random selection 4)	862	1088	3654
GSE123892, GSE151352, TCGA-GBM (random selection 5)	845	1078	3695
GSE123892, GSE151352, TCGA-GBM (random selection 6)	863	1107	3689
GSE123892, GSE151352, TCGA-GBM (random selection 7)	876	1062	3644
GSE123892, GSE151352, TCGA-GBM (random selection 8)	887	1094	3697
GSE123892, GSE151352, TCGA-GBM (random selection 9)	830	1097	3702
GSE123892, GSE151352, TCGA-GBM (random selection 10)	911	1090	3605

b. For DEGs with the mismatched direction of expression across 3 studies			
Datasets	DEGs Present in 1	DEGs Present in 2	DEGs Present in 3
GSE123892, GSE151352, TCGA-GBM (all samples)	0	52	181
GSE123892, GSE151352, TCGA-GBM (random selection 1)	0	26	140
GSE123892, GSE151352, TCGA-GBM (random selection 2)	0	41	171
GSE123892, GSE151352, TCGA-GBM (random selection 3)	0	38	149
GSE123892, GSE151352, TCGA-GBM (random selection 4)	0	34	166
GSE123892, GSE151352, TCGA-GBM (random selection 5)	0	28	154
GSE123892, GSE151352, TCGA-GBM (random selection 6)	0	33	140
GSE123892, GSE151352, TCGA-GBM (random selection 7)	0	39	173
GSE123892, GSE151352, TCGA-GBM (random selection 8)	0	30	179
GSE123892, GSE151352, TCGA-GBM (random selection 9)	0	39	165
GSE123892, GSE151352, TCGA-GBM (random selection 10)	0	34	164

Supplementary Table 5. Number of DEGs identified by the fused inverse-normal (FIN) method in the GBM data application for both scenarios and number of these DEGs present in one, two or all three datasets considered. **a.** For DEGs with the same direction of expression across all three studies. **b.** For DEGs with conflicting direction of expression across studies

a. For DEGs with the same direction of expression across all 3 studies			
Datasets	DEGs Present in 1	DEGs Present in 2	DEGs Present in 3
GSE123892, GSE151352, TCGA-GBM (all samples)	1359	1083	3461
GSE123892, GSE151352, TCGA-GBM (random selection 1)	911	1080	3508
GSE123892, GSE151352, TCGA-GBM (random selection 2)	933	1077	3475
GSE123892, GSE151352, TCGA-GBM (random selection 3)	931	1070	3457
GSE123892, GSE151352, TCGA-GBM (random selection 4)	957	1077	3476
GSE123892, GSE151352, TCGA-GBM (random selection 5)	931	1073	3536
GSE123892, GSE151352, TCGA-GBM (random selection 6)	935	1096	3540
GSE123892, GSE151352, TCGA-GBM (random selection 7)	962	1051	3460
GSE123892, GSE151352, TCGA-GBM (random selection 8)	978	1101	3509
GSE123892, GSE151352, TCGA-GBM (random selection 9)	912	1078	3526
GSE123892, GSE151352, TCGA-GBM (random selection 10)	988	1076	3436

b. For DEGs with the mismatched direction of expression across 3 studies			
Datasets	DEGs Present in 1	DEGs Present in 2	DEGs Present in 3
GSE123892, GSE151352, TCGA-GBM (all samples)	0	53	182
GSE123892, GSE151352, TCGA-GBM (random selection 1)	0	26	140
GSE123892, GSE151352, TCGA-GBM (random selection 2)	0	41	171
GSE123892, GSE151352, TCGA-GBM (random selection 3)	0	38	149

GSE123892, GSE151352, TCGA-GBM (random selection 4)	0	34	166
GSE123892, GSE151352, TCGA-GBM (random selection 5)	0	28	154
GSE123892, GSE151352, TCGA-GBM (random selection 6)	0	32	140
GSE123892, GSE151352, TCGA-GBM (random selection 7)	0	39	172
GSE123892, GSE151352, TCGA-GBM (random selection 8)	0	30	179
GSE123892, GSE151352, TCGA-GBM (random selection 9)	0	39	165
GSE123892, GSE151352, TCGA-GBM (random selection 10)	0	34	164

Supplementary Table 6. IPA canonical pathways for **a.** up and **b.** down-regulated DEGs present in all three GBM datasets and identified by the FIN method. Ratio denotes the number of DEGs enriched in a pathway to the total number of genes in that pathway.

Ingenuity Canonical Pathways	-log(BH p-value)	Ratio	z-score
a. Pathways from up-regulated DEGs			
Kinetochores Metaphase Signaling Pathway	14.1	0.376	3.413
Hepatic Fibrosis Signaling Pathway	12.4	0.205	7.714
Osteoarthritis Pathway	11.1	0.241	5.126
Cell Cycle Control of Chromosomal Replication	8.23	0.393	4.69
Role of BRCA1 in DNA Damage Response	7.88	0.325	2.837
IL-8 Signaling	7.36	0.215	5.84
Tumor Microenvironment Pathway	6.56	0.216	4.867
Estrogen-mediated S-phase Entry	6.32	0.5	2.496
Death Receptor Signaling	6.19	0.272	3.4
GP6 Signaling Pathway	6.17	0.244	5.385
Acute Phase Response Signaling	5.98	0.206	4.596
Colorectal Cancer Metastasis Signaling	5.9	0.182	5.376
Dendritic Cell Maturation	5.76	0.201	5.831
Glioblastoma Multiforme Signaling	5.53	0.206	4.158
ILK Signaling	5.43	0.195	4.7
FAT10 Cancer Signaling Pathway	5.43	0.348	2
EIF2 Signaling	5.35	0.183	2.711
Senescence Pathway	5.32	0.171	1.021
Type I Diabetes Mellitus Signaling	5.27	0.234	3.441

Regulation Of The Epithelial Mesenchymal Transition By Growth Factors Pathway	5.16	0.191	5.667
Production of Nitric Oxide and Reactive Oxygen Species in Macrophages	5.12	0.19	5.24
Neuroinflammation Signaling Pathway	5.03	0.163	6.112
HOTAIR Regulatory Pathway	5.01	0.2	3.772
Cyclins and Cell Cycle Regulation	5	0.259	1.528
Signaling by Rho Family GTPases	4.87	0.17	5.745
Role of PKR in Interferon Induction and Antiviral Response	4.84	0.22	3.411
Leukocyte Extravasation Signaling	4.58	0.181	3.889
Pancreatic Adenocarcinoma Signaling	4.5	0.22	2.84
Glioma Signaling	4.44	0.218	3.317
HIF1 α Signaling	4.43	0.176	4.333
Tec Kinase Signaling	4.39	0.185	4.796
p53 Signaling	4.28	0.224	0.535
Inhibition of Angiogenesis by TSP1	4.26	0.353	2.53
Regulation of Cellular Mechanics by Calpain Protease	3.95	0.243	1.732
IL-6 Signaling	3.94	0.198	4.491
STAT3 Pathway	3.87	0.193	2.982
Bladder Cancer Signaling	3.86	0.216	2
TNFR1 Signaling	3.76	0.28	3.051
Ovarian Cancer Signaling	3.67	0.187	3.317
Apoptosis Signaling	3.67	0.21	1.789
BEX2 Signaling Pathway	3.6	0.228	2.828
Breast Cancer Regulation by Stathmin1	3.57	0.125	6.215
Mitotic Roles of Polo-Like Kinase	3.54	0.242	1.069
MSP-RON Signaling In Cancer Cells Pathway	3.54	0.187	4.6
Aryl Hydrocarbon Receptor Signaling	3.51	0.182	0.894
Systemic Lupus Erythematosus In B Cell Signaling Pathway	3.47	0.149	4.841
ATM Signaling	3.43	0.206	0.775
TREM1 Signaling	3.42	0.227	4.123
Induction of Apoptosis by HIV1	3.42	0.246	2.84
NF- κ B Signaling	3.42	0.168	4.747
Notch Signaling	3.25	0.297	1.414
Myc Mediated Apoptosis Signaling	3.23	0.26	2.496
Sphingosine-1-phosphate Signaling	3.21	0.188	1.706
Fcy Receptor-mediated Phagocytosis in Macrophages and Monocytes	3.18	0.202	4.359
Glioma Invasiveness Signaling	3.09	0.219	2.5
Th2 Pathway	3.09	0.176	1.732

Crosstalk between Dendritic Cells and Natural Killer Cells	3.04	0.202	3.464
Cytotoxic T Lymphocyte-mediated Apoptosis of Target Cells	2.94	0.294	2.449
Regulation Of The Epithelial Mesenchymal Transition In Development Pathway	2.87	0.202	3.742
TWEAK Signaling	2.84	0.286	1.897
Integrin Signaling	2.84	0.15	4.914
Tumoricidal Function of Hepatic Natural Killer Cells	2.73	0.333	2.646
Ephrin Receptor Signaling	2.72	0.153	3.5
NER Pathway	2.71	0.184	2.828
Role of Pattern Recognition Receptors in Recognition of Bacteria and Viruses	2.71	0.162	3.742
Wnt/ β -catenin Signaling	2.67	0.156	1.4
Complement System	2.67	0.27	1.414
Protein Kinase A Signaling	2.52	0.125	0.686
fMLP Signaling in Neutrophils	2.5	0.172	3.207
LPS/IL-1 Mediated Inhibition of RXR Function	2.47	0.142	0.943
Actin Cytoskeleton Signaling	2.41	0.141	4.2
GM-CSF Signaling	2.36	0.2	2.496
VDR/RXR Activation	2.36	0.192	0.707
HGF Signaling	2.34	0.167	3.357
HMGB1 Signaling	2.32	0.152	4.583
Small Cell Lung Cancer Signaling	2.32	0.197	2.333
Th1 Pathway	2.31	0.165	2.84
Semaphorin Neuronal Repulsive Signaling Pathway	2.29	0.158	0.853
PI3K/AKT Signaling	2.28	0.146	2.673
Acute Myeloid Leukemia Signaling	2.23	0.18	2.53
TNFR2 Signaling	2.13	0.267	1.89
Role of NFAT in Regulation of the Immune Response	2.12	0.144	4.472
mTOR Signaling	2.1	0.138	3.464
Glutathione Redox Reactions I	2.1	0.292	2.646
Androgen Signaling	2.09	0.154	1.667
Cardiac Hypertrophy Signaling (Enhanced)	2.09	0.115	6.934
Toll-like Receptor Signaling	2.07	0.184	2.496
iNOS Signaling	2.07	0.222	2.828
Mouse Embryonic Stem Cell Pluripotency	2	0.165	3.638

Ingenuity Canonical Pathways	-log(BH p-value)	Ratio	z-score
b. Pathways from down-regulated DEGs			
Synaptogenesis Signaling Pathway	24.5	0.288	-8.013
Endocannabinoid Neuronal Synapse Pathway	16	0.359	-4.727

Role of NFAT in Cardiac Hypertrophy	14.1	0.271	-6.456
Opioid Signaling Pathway	13	0.247	-6.04
GNRH Signaling	10.2	0.26	-5.477
Calcium Signaling	10.2	0.243	-6.091
G Beta Gamma Signaling	9.03	0.287	-5.396
Dopamine-DARPP32 Feedback in cAMP Signaling	8.81	0.252	-4.902
Synaptic Long Term Depression	8.38	0.233	-5.555
GPCR-Mediated Nutrient Sensing in Enteroendocrine Cells	8.26	0.286	-5.303
Neuropathic Pain Signaling In Dorsal Horn Neurons	8.22	0.297	-5.477
Reelin Signaling in Neurons	7.97	0.27	-5.657
Netrin Signaling	7.85	0.354	-4.796
Synaptic Long Term Potentiation	7.38	0.256	-5.209
CCR5 Signaling in Macrophages	7.09	0.287	-3.464
Melatonin Signaling	6.93	0.319	-3.545
CXCR4 Signaling	6.58	0.222	-4.041
Protein Kinase A Signaling	6.55	0.165	-2.84
Signaling by Rho Family GTPases	6.44	0.19	-5.24
Corticotropin Releasing Hormone Signaling	6.17	0.228	-1.095
Cardiac Hypertrophy Signaling	5.91	0.188	-5.754
Apelin Endothelial Signaling Pathway	5.85	0.243	-3.657
Sperm Motility	5.57	0.188	-5.099
Thrombin Signaling	5.54	0.192	-4.271
Nitric Oxide Signaling in the Cardiovascular System	5.54	0.253	-4.491
Cardiac β -adrenergic Signaling	5.53	0.22	-2.837
Androgen Signaling	5.38	0.221	-4.583
α -Adrenergic Signaling	5.25	0.25	-3.873
Superpathway of Inositol Phosphate Compounds	5.24	0.191	-6.083
Type II Diabetes Mellitus Signaling	4.99	0.211	-3.051
G α q Signaling	4.94	0.203	-5.196
Glutamate Receptor Signaling	4.75	0.298	-1.89
cAMP-mediated signaling	4.6	0.175	-5.096
Huntington's Disease Signaling	4.58	0.173	-1.706
nNOS Signaling in Neurons	4.57	0.319	-3
3-phosphoinositide Biosynthesis	4.5	0.193	-5.568
White Adipose Tissue Browning Pathway	4.44	0.209	-4.426
CREB Signaling in Neurons	4.42	0.134	-7.778
Insulin Secretion Signaling Pathway	4.3	0.168	-5.778
Fc γ RIIB Signaling in B Lymphocytes	4.27	0.253	-2.449
Renin-Angiotensin Signaling	4.22	0.212	-4.583
Adrenomedullin signaling pathway	4.18	0.178	-5.657
D-myo-inositol-5-phosphate Metabolism	4.18	0.191	-5.385
14-3-3-mediated Signaling	4.15	0.205	-3.838
Endothelin-1 Signaling	3.84	0.176	-4.131
Phospholipase C Signaling	3.8	0.158	-4.914
Relaxin Signaling	3.74	0.187	-3.606
D-myo-inositol (1,4,5,6)-Tetrakisphosphate Biosynthesis	3.74	0.19	-5.099

D-myo-inositol (3,4,5,6)-tetrakisphosphate Biosynthesis	3.74	0.19	-5.099
Cholecystokinin/Gastrin-mediated Signaling	3.74	0.202	-4.583
P2Y Purigenic Receptor Signaling Pathway	3.72	0.197	-4.264
Apelin Cardiomyocyte Signaling Pathway	3.58	0.212	-4.583
CDK5 Signaling	3.49	0.204	-2.4
CCR3 Signaling in Eosinophils	3.46	0.194	-3.742
3-phosphoinositide Degradation	3.46	0.179	-5.196
Chemokine Signaling	3.41	0.225	-3.638
Aldosterone Signaling in Epithelial Cells	3.38	0.177	-4.359
Cardiac Hypertrophy Signaling (Enhanced)	3.13	0.129	-7.366
PKC θ Signaling in T Lymphocytes	3.13	0.174	-3.742
Endocannabinoid Developing Neuron Pathway	3.11	0.191	-1.606
Sphingosine-1-phosphate Signaling	3.01	0.188	-2.828
ErbB Signaling	2.99	0.202	-4.243
UVB-Induced MAPK Signaling	2.9	0.25	-3.606
p70S6K Signaling	2.82	0.178	-3.13
Rac Signaling	2.82	0.182	-4.243
Tec Kinase Signaling	2.75	0.162	-4.123
RhoA Signaling	2.73	0.179	-3.13
Pregnenolone Biosynthesis	2.73	0.462	-2.449
G α s Signaling	2.73	0.187	-3.3
IL-1 Signaling	2.69	0.196	-1.89
fMLP Signaling in Neutrophils	2.69	0.181	-4.243
Ephrin B Signaling	2.52	0.208	-3.317
HGF Signaling	2.51	0.175	-4.243
RhoGDI Signaling	2.51	0.153	2.828
Ephrin Receptor Signaling	2.51	0.153	-4.583
GPCR-Mediated Integration of Enteroendocrine Signaling Exemplified by an L Cell	2.47	0.205	-0.258
IL-8 Signaling	2.44	0.15	-4.796
Leptin Signaling in Obesity	2.41	0.203	-2.236
Histidine Degradation VI	2.4	0.4	-2.449
B Cell Receptor Signaling	2.31	0.151	-4.041
Role of NFAT in Regulation of the Immune Response	2.17	0.149	-3.838
PI3K Signaling in B Lymphocytes	2.11	0.159	-4.472
Ubiquinol-10 Biosynthesis (Eukaryotic)	2.09	0.353	-2.449
ERK/MAPK Signaling	2.09	0.144	-3
Amyotrophic Lateral Sclerosis Signaling	2.05	0.175	-2.111
RANK Signaling in Osteoclasts	2.04	0.18	-4
Neuroinflammation Signaling Pathway	2.03	0.13	-2.785
UVA-Induced MAPK Signaling	2.01	0.173	-3.464

Supplementary Table 7. IPA upstream regulator analysis results for **a.** up and **b.** down-regulated DEGs present in all three GBM datasets and identified by the FIN method.

Upstream Regulator	mean logFC	Molecule Type	Activation z-score	P-value overlap	BH p-value
a. Upstream regulators for up-regulated DEGs					
TGFB1	1.041	growth factor	8.971	2.51E-88	2.08E-84
TP53	2.208	transcription regulator	3.96	9.95E-80	4.14E-76
ERBB2	1.26	kinase	7.269	2.60E-66	3.60E-63
MYC	2.687	transcription regulator	4.855	4.37E-62	4.55E-59
CDKN1A	2.457	kinase	-4.091	2.34E-56	1.77E-53
NFKBIA	1.272	transcription regulator	3.344	1.80E-43	7.47E-41
FOXM1	4.83	transcription regulator	7.238	5.80E-39	1.79E-36
EGFR	4.605	kinase	5.001	9.51E-37	2.64E-34
CCND1	1.251	transcription regulator	4.578	2.88E-33	5.44E-31
YAP1	1.162	transcription regulator	5.297	7.46E-32	1.29E-29
TWIST1	1.889	transcription regulator	4.192	7.09E-30	1.02E-27
E2F1	1.146	transcription regulator	5.853	1.04E-28	1.35E-26
TBX2	3.103	transcription regulator	4.433	7.35E-28	8.86E-26
NUPR1	1.918	transcription regulator	-3.927	1.43E-26	1.51E-24
AR	2.049	ligand-dependent nuclear receptor	3.669	1.19E-25	1.15E-23
JUN	1.495	transcription regulator	5.72	2.87E-25	2.57E-23
NR1H3	1.074	ligand-dependent nuclear receptor	2.203	1.23E-24	1.05E-22
AKT1	1.066	kinase	4.256	3.66E-24	2.92E-22
VEGFA	3.776	growth factor	6.513	1.21E-23	9.28E-22
SPI1	1.254	transcription regulator	1.876	1.63E-23	1.22E-21
TCF3	1.887	transcription regulator	-0.806	9.61E-23	6.50E-21
FAS	1.754	transmembrane receptor	-2.084	2.13E-22	1.42E-20
TGFB2	1.198	growth factor	3.424	5.11E-22	3.32E-20
CD44	2.568	other	4.541	2.28E-20	1.27E-18
APOE	1.358	transporter	-4.791	2.73E-19	1.39E-17
IRF1	2.009	transcription regulator	5.486	9.97E-19	4.74E-17
CEBPB	1.262	transcription regulator	5.281	1.01E-18	4.77E-17
FN1	2.971	enzyme	5.104	2.56E-17	1.10E-15
CDK4	3.341	kinase	0.469	6.10E-17	2.51E-15
ANGPT2	3.221	growth factor	6.136	6.54E-17	2.68E-15
CCN2	1.487	growth factor	4.292	5.92E-16	2.16E-14
E2F2	5.191	transcription regulator	2.494	8.16E-16	2.95E-14
EZH2	3.461	transcription regulator	0.551	8.72E-16	3.14E-14

NOTCH3	2.12	transcription regulator	4.045	1.01E-15	3.60E-14
IRF7	1.324	transcription regulator	6.854	1.06E-15	3.73E-14
RBL1	1.244	transcription regulator	-4.344	4.95E-15	1.62E-13
F2R	3.98	G-protein coupled receptor	5.338	6.13E-15	2.00E-13
BIRC5	4.835	other	-1.709	1.25E-14	3.99E-13
S100A9	3.908	other	3.047	1.42E-14	4.51E-13
CD40	1.101	transmembrane receptor	4.744	1.43E-14	4.51E-13
NAMPT	2.502	cytokine	2.682	1.61E-14	5.07E-13
MYBL2	6.787	transcription regulator	2.79	2.89E-14	8.80E-13
ABCB4	2.036	transporter	-4.078	4.01E-14	1.18E-12
JAG1	2.726	growth factor	4.426	7.45E-14	2.14E-12
COL18A1	1.65	other	-4.828	7.84E-14	2.22E-12
PLK1	2.524	kinase	-2.02	8.98E-14	2.51E-12
ACVRL1	1.465	kinase	-0.024	1.80E-13	4.82E-12
S100A6	2.611	transporter	0.943	2.05E-13	5.45E-12
CIP2A	1.493	other	-1.763	2.76E-13	7.26E-12
HOXA10	7.693	transcription regulator	-2.33	2.84E-13	7.44E-12
RARA	1.599	ligand-dependent nuclear receptor	3.454	3.26E-13	8.42E-12
TEAD4	2.789	transcription regulator	4.204	3.84E-13	9.81E-12
IL33	1.493	cytokine	5.613	4.17E-13	1.06E-11
DCN	1.381	other	-1.12	7.13E-13	1.77E-11
S100A8	4.872	other	2.378	7.63E-13	1.89E-11
ID3	2.405	transcription regulator	-0.307	1.94E-12	4.46E-11
BCL6	1.086	transcription regulator	-1.729	4.74E-12	1.04E-10
CCN1	2.124	other	3.663	7.29E-12	1.56E-10
MYD88	1.788	other	6.715	1.37E-11	2.83E-10
TREM1	4.669	transmembrane receptor	3.236	2.24E-11	4.50E-10
TNFSF13B	1.681	cytokine	3.489	2.32E-11	4.64E-10
ENG	1.746	transmembrane receptor	0.342	2.82E-11	5.59E-10
HMOX1	2.464	enzyme	-1.425	4.55E-11	8.73E-10
TEAD2	3.281	transcription regulator	4	7.47E-11	1.40E-09
SPP1	1.055	cytokine	5.002	9.83E-11	1.79E-09
IL10RA	1.235	transmembrane receptor	-0.431	1.01E-10	1.84E-09
SMAD1	1.086	transcription regulator	3.773	1.03E-10	1.87E-09
CXCR4	2.307	G-protein coupled receptor	2.791	1.18E-10	2.12E-09
ETS1	1.474	transcription regulator	4.918	1.43E-10	2.55E-09

NOX4	2.202	enzyme	3.208	2.56E-10	4.46E-09
MAP3K1	1.417	kinase	4.376	2.69E-10	4.66E-09
ATF3	1.086	transcription regulator	-1.834	3.38E-10	5.79E-09
THBS1	2.392	other	0.938	4.76E-10	8.00E-09
WWTR1	2.559	transcription regulator	2.275	5.97E-10	9.83E-09
GLIS2	1.085	transcription regulator	-3.45	6.95E-10	1.14E-08
RUNX3	1.993	transcription regulator	-3.767	8.63E-10	1.39E-08
KLF6	1.287	transcription regulator	1.665	9.32E-10	1.49E-08
TFAP2A	3.639	transcription regulator	-1.105	9.69E-10	1.54E-08
PLAU	4.022	peptidase	2.262	1.38E-09	2.14E-08
CHEK1	2.576	kinase	1.233	1.75E-09	2.67E-08
PTGER4	1.554	G-protein coupled receptor	-1.729	2.73E-09	4.06E-08
ETV4	3.275	transcription regulator	3.774	3.55E-09	5.16E-08
S100A4	3.034	other	2.341	4.52E-09	6.43E-08
MMP9	6.815	peptidase	3.108	5.04E-09	7.08E-08
TLR3	1.497	transmembrane receptor	5.937	5.38E-09	7.53E-08
TEAD3	2.377	transcription regulator	3.771	6.51E-09	9.03E-08
SOX2	1.572	transcription regulator	0.781	7.82E-09	1.07E-07
TNFRSF1A	1.995	transmembrane receptor	1.079	1.15E-08	1.52E-07
ANXA2	3.997	other	-1.574	1.25E-08	1.64E-07
SNAI2	2.56	transcription regulator	2.345	1.34E-08	1.75E-07
HMGA1	1.256	transcription regulator	1.163	1.44E-08	1.86E-07
ITGA5	2.844	transmembrane receptor	2.102	1.47E-08	1.90E-07
PDGFC	1.867	growth factor	3.388	1.79E-08	2.30E-07
TYROBP	1.505	transmembrane receptor	2.2	2.24E-08	2.83E-07
DLL4	1.581	other	-0.357	2.27E-08	2.86E-07
PRDM1	1.411	transcription regulator	-1.626	2.51E-08	3.15E-07
SPARC	2.132	other	-0.419	2.68E-08	3.36E-07
ZEB1	1.431	transcription regulator	1.684	4.32E-08	5.24E-07
NCF1	1.26	enzyme	2.905	5.57E-08	6.62E-07
IGFBP2	4.882	other	2.823	6.06E-08	7.13E-07
SOX4	2.495	transcription regulator	3.934	6.18E-08	7.26E-07
TIMP1	3.632	cytokine	1.604	1.11E-07	1.24E-06
E2F5	1.566	transcription regulator	2	1.15E-07	1.28E-06
TLR2	1.287	transmembrane receptor	1.861	1.60E-07	1.74E-06

CXCL8	3.465	cytokine	2.976	2.01E-07	2.15E-06
ASCL1	1.684	transcription regulator	2.383	2.03E-07	2.16E-06
PARP9	1.68	enzyme	2.373	2.29E-07	2.42E-06
NEDD9	1.814	other	1.973	2.29E-07	2.42E-06
ZMYND10	1.329	other	-0.342	2.45E-07	2.55E-06
ACKR3	1.907	G-protein coupled receptor	2.027	2.45E-07	2.55E-06
MSTN	1.995	growth factor	0.366	2.90E-07	2.98E-06
SPHK1	1.69	kinase	1.646	3.16E-07	3.22E-06
GMNN	1.505	transcription regulator	-3.748	3.20E-07	3.26E-06
WNT5A	1.846	cytokine	1.597	3.22E-07	3.27E-06
CTSB	1.196	peptidase	2.408	3.31E-07	3.35E-06
LGALS3	3.025	other	0.747	3.35E-07	3.39E-06
BAX	1.466	transporter	2.256	3.61E-07	3.62E-06
POSTN	6.219	other	2.589	3.61E-07	3.62E-06
DDB2	1.301	other	0.354	5.65E-07	5.46E-06
IFIH1	1.048	enzyme	3.142	6.04E-07	5.77E-06
CDK2	2.938	kinase	2.496	7.22E-07	6.82E-06
ACTL6A	1.54	other	0.905	8.51E-07	7.96E-06
MAP3K14	1.231	kinase	2.881	8.79E-07	8.19E-06
NFKB2	1.33	transcription regulator	3.218	1.09E-06	1.01E-05
RUNX1	1.627	transcription regulator	1.428	1.10E-06	1.01E-05
OSMR	2.989	transmembrane receptor	1.4	1.13E-06	1.04E-05
CASP3	1.189	peptidase	1.249	1.32E-06	1.20E-05
GDF15	5.161	growth factor	0.765	1.48E-06	1.33E-05
PGF	2.975	growth factor	2.245	1.66E-06	1.46E-05
PLAUR	2.196	transmembrane receptor	2.61	1.66E-06	1.46E-05
MUC1	2.76	other	2.782	1.87E-06	1.63E-05
BCL6B	1.668	transcription regulator	1.309	1.87E-06	1.63E-05
ADAMTS12	2.3	peptidase	-3.138	1.88E-06	1.63E-05
PTGS1	2.051	enzyme	1.5	2.30E-06	1.97E-05
TRAF3IP2	1.532	other	3.939	2.71E-06	2.29E-05
HSPB1	1.863	other	0.921	2.95E-06	2.47E-05
PDGFRA	2.422	kinase	2.21	3.02E-06	2.51E-05
TYMS	1.54	enzyme	-2.213	3.10E-06	2.55E-05
CEBPD	2.348	transcription regulator	0.231	3.11E-06	2.56E-05
ICAM1	2.224	transmembrane receptor	3.418	3.40E-06	2.79E-05
MEX3A	3.168	other	1.387	3.80E-06	3.09E-05
MMP2	3.159	peptidase	2.053	3.80E-06	3.09E-05
ADAM12	2.471	peptidase	-0.269	4.19E-06	3.40E-05
ANXA1	3.445	enzyme	-1.1	4.31E-06	3.48E-05

HLX	1.738	transcription regulator	-1.66	4.31E-06	3.48E-05
NT5E	1.606	phosphatase	-1.134	5.34E-06	4.24E-05
GPX1	1.407	enzyme	-3.532	5.80E-06	4.59E-05
IGFBP7	2.448	transporter	-0.174	5.91E-06	4.64E-05
EDNRA	2.101	transmembrane receptor	2.828	5.91E-06	4.64E-05
ETV1	2.044	transcription regulator	2.158	6.60E-06	5.13E-05
TGFB1I1	3.679	transcription regulator	0.452	6.60E-06	5.13E-05
SAMSN1	1.112	other	4.583	6.61E-06	5.13E-05
CIITA	1.126	transcription regulator	1.576	7.27E-06	5.59E-05
LATS2	1.081	kinase	0.971	7.27E-06	5.59E-05
PIM1	1.032	kinase	2.179	7.28E-06	5.60E-05
AURKB	5.485	kinase	-1.177	9.02E-06	6.78E-05
IFI16	1.477	transcription regulator	3.262	9.50E-06	7.12E-05
KDR	1.413	kinase	1.105	1.02E-05	7.60E-05
SHC1	1.751	other	-0.967	1.60E-05	0.000115
PSMB9	1.808	peptidase	0.391	1.67E-05	0.000118
SERPINH1	3.581	other	2.401	1.67E-05	0.000118
CPXM1	4.813	peptidase	2.236	1.74E-05	0.000121
LEF1	1.707	transcription regulator	1.929	1.90E-05	0.000132
ZNF217	1.274	transcription regulator	-1.846	2.03E-05	0.00014
AIF1	1.007	other	2.607	2.16E-05	0.000149
SPRY2	1.039	other	-0.992	2.27E-05	0.000155
ARHGAP31	1.041	other	-0.905	2.81E-05	0.000189
SOCS3	2.869	phosphatase	-1.99	3.27E-05	0.000217
TRIB3	2.785	kinase	-1.897	3.29E-05	0.000218
TNFAIP3	1.782	enzyme	-2.028	3.63E-05	0.000237
PLAT	2.471	peptidase	2.921	3.86E-05	0.000251
AEBP1	2.812	peptidase	-0.403	3.89E-05	0.000252
CYBA	1.593	enzyme	2.414	3.89E-05	0.000252
RUVBL1	1.297	transcription regulator	1.808	3.92E-05	0.000252
SNHG1	1.044	other	-0.243	3.92E-05	0.000252
LAMC1	2.891	other	-2.616	4.03E-05	0.000256
ID4	1.659	transcription regulator	-1.951	4.03E-05	0.000256
HOXA7	7.114	transcription regulator	2.547	4.67E-05	0.000294
C3AR1	1.143	G-protein coupled receptor	2.107	5.03E-05	0.000317
EPHA2	2.476	kinase	1.977	5.20E-05	0.000326
NGFR	2.284	transmembrane receptor	-0.328	5.22E-05	0.000326
TNFRSF1B	1.187	transmembrane receptor	3.29	5.64E-05	0.000348

MCM7	1.516	enzyme	NA	5.68E-05	0.000348
CKS1B	1.363	kinase	2.215	5.68E-05	0.000348
C3	1.272	peptidase	2.563	6.00E-05	0.000367
C1QA	2.385	other	1.237	6.51E-05	0.000395
CRNDE	2.876	other	2.37	6.99E-05	0.000424
HAS2	3.55	enzyme	0.808	7.98E-05	0.000475
CDK1	3.762	kinase	2.213	8.07E-05	0.000478
RND3	2.011	enzyme	1.945	8.07E-05	0.000478
LTBR	1.001	transmembrane receptor	1.508	8.09E-05	0.000479
MAPK7	1.248	kinase	1.631	8.83E-05	0.00052
CLU	1.038	other	0.913	8.92E-05	0.000523
HOXD10	8.605	transcription regulator	1.343	9.14E-05	0.000534
SOX11	3.377	transcription regulator	1.646	9.89E-05	0.000575
INHBB	1.78	growth factor	2.8	0.000108	0.000628
EFNA2	1.755	kinase	-2.673	0.000109	0.000628
ID1	1.214	transcription regulator	2.043	0.000109	0.00063
MAFB	1.242	transcription regulator	1.323	0.000115	0.000665
COL1A1	4.721	other	1.934	0.000117	0.000667
GAS2L3	3.14	other	-2.63	0.000117	0.000667
CBX3	1.288	transcription regulator	NA	0.000121	0.000689
PRKD1	1.199	kinase	3.532	0.000126	0.000714
SMO	2.739	G-protein coupled receptor	NA	0.000135	0.00076
DES	2.527	other	-1.98	0.000142	0.000789
ELN	2.609	other	0.896	0.000149	0.000822
CTSS	1.594	peptidase	1.026	0.000151	0.000834
MEOX2	4.66	transcription regulator	-2.474	0.000156	0.000859
RIPK1	1.161	kinase	0.632	0.00018	0.000978
MELK	5.434	kinase	1.896	0.000184	0.00098
FZD7	2.772	G-protein coupled receptor	1	0.000184	0.00098
BRCA2	2.764	transcription regulator	-1.154	0.000184	0.00098
HELLS	1.894	enzyme	2	0.000185	0.00098
NEDD4	1.549	enzyme	-1.671	0.000185	0.00098
PTTG1	3.247	transcription regulator	-0.238	0.000215	0.00113
STK40	1.112	kinase	1.589	0.000253	0.00131
GAS5	1.03	other	-1.604	0.000253	0.00131
LOX	4.548	enzyme	1.906	0.000253	0.00131
PDGFRB	1.307	kinase	0.842	0.000258	0.00133
ITGB2	1.448	transmembrane receptor	0.971	0.000278	0.00143
EFNA4	1.655	kinase	-3.317	0.00032	0.00161

HEY1	1.792	transcription regulator	-0.97	0.000354	0.00176
GAPDH	1.067	enzyme	-2.109	0.000355	0.00177
DPP4	2.169	peptidase	0.283	0.000399	0.00198
SULF2	1.281	enzyme	1.391	0.000415	0.00204
ACTB	1.024	other	0.956	0.000415	0.00204
BIRC3	1.523	enzyme	-0.216	0.000484	0.00235
USP18	1.777	peptidase	-2.959	0.000487	0.00235
MECOM	1.255	transcription regulator	0.577	0.000487	0.00235
CD14	2.631	transmembrane receptor	3.24	0.000497	0.00236
TIMP3	1.46	other	-2.354	0.000507	0.0024
MKI67	5.201	other	1.216	0.000516	0.00242
PARP14	1.209	enzyme	1.387	0.000556	0.00257
ITGA4	2.774	transmembrane receptor	-0.129	0.000556	0.00257
ATF5	1.443	transcription regulator	1.969	0.000556	0.00257
CISH	2.232	other	-1.175	0.000598	0.00272
CGAS	1.247	enzyme	2.815	0.000651	0.00294
CDH2	1.052	other	0.577	0.000655	0.00294
NRP1	2.015	transmembrane receptor	0.128	0.000655	0.00294
ADM	3.417	other	-2.099	0.000735	0.00328
MMP14	3.434	peptidase	-1.195	0.000807	0.00359
NLRC5	1.94	transcription regulator	1.926	0.000832	0.00368
PROCR	1.694	other	0.788	0.000862	0.0038
BGN	1.918	other	0.239	0.000862	0.0038
CALR	1.239	transcription regulator	1.525	0.000902	0.00396
CD36	1.975	transmembrane receptor	4.202	0.000908	0.00398
MCL1	1.314	transporter	0.871	0.000954	0.00414
H1-2	2.235	other	-0.42	0.000978	0.00423
DNASE2	1.292	enzyme	-2.784	0.00102	0.0044
SOX9	1.516	transcription regulator	2.165	0.00103	0.00444
CCR1	1.03	G-protein coupled receptor	0.895	0.00112	0.00476
TMPO	1.043	other	2	0.00113	0.00476
LGALS1	2.065	other	2.275	0.00138	0.00574
TNFAIP6	1.941	other	1.915	0.00152	0.00624
HNRNPAB	1.296	enzyme	2	0.00153	0.00624
YBX1	1.7	transcription regulator	1.719	0.00169	0.00687
EBF1	1.316	transcription regulator	3.057	0.00197	0.00772
AURKA	2.84	kinase	1.023	0.00198	0.00772
IGFBP5	2.229	other	2.007	0.00201	0.00778
ACE	2.002	peptidase	0.816	0.00201	0.00778

HOXA5	7.06	transcription regulator	2.361	0.00201	0.00778
HAND2	5.899	transcription regulator	-0.444	0.00205	0.00795
EFEMP1	2.47	enzyme	-1.982	0.00212	0.00807
TSPO	1.285	transmembrane receptor	-1	0.00212	0.00807
PLA2G5	2.165	enzyme	1.98	0.00212	0.00807
NR5A2	4.148	ligand-dependent nuclear receptor	0.978	0.00246	0.00929
SOX6	1.243	transcription regulator	0.862	0.0026	0.00976

Upstream Regulator	mean logFC	Molecule Type	Activation z-score	P-value overlap	BH p-value
b. Upstream regulators for down-regulated DEGs					
TCF7L2	NA	transcription regulator	-9.736	9.79E-31	4.22E-27
MAPT	-1.398	other	0.728	2.66E-24	5.74E-21
levodopa	NA	chemical - endogenous mammalian	-3.748	2.00E-19	2.88E-16
HTT	NA	transcription regulator	1.919	7.36E-17	6.91E-14
FMR1	NA	translation regulator	5.211	8.02E-17	6.91E-14
SNCA	-4.209	enzyme	-1.176	3.76E-15	2.52E-12
REST	NA	transcription regulator	4.284	4.09E-15	2.52E-12
BDNF	NA	growth factor	-5.649	6.51E-12	3.51E-09
DSCAML1	-2.164	other	-3.651	9.02E-12	4.32E-09
HDAC4	NA	transcription regulator	-0.863	1.16E-10	4.98E-08
DSCAM	NA	other	-4.163	2.22E-10	8.70E-08
MKNK1	NA	kinase	-5.477	3.02E-10	1.08E-07
topotecan	NA	chemical drug	4.753	4.85E-10	1.50E-07
CREB1	NA	transcription regulator	0.459	4.86E-10	1.50E-07
PHF21A	NA	other	-2.51	1.43E-09	4.12E-07
MECP2	NA	transcription regulator	-2.411	6.96E-09	1.76E-06
tetrodotoxin	NA	chemical drug	2.219	1.34E-08	3.21E-06
Calmodulin	NA	group	-2.059	1.87E-08	4.25E-06
PSEN1	-1.141	peptidase	-0.722	4.16E-08	8.96E-06
GRIN3A	NA	ion channel	5.292	8.98E-08	1.84E-05
DMD	NA	other	-1.32	3.12E-07	6.11E-05
APP	-1.079	other	0.476	1.92E-06	0.000359
NFASC	-2.903	other	-2.952	3.81E-06	0.000684
tazemetostat	NA	chemical drug	-2.929	4.89E-06	0.000842
SLC30A3	NA	transporter	-2.433	1.96E-05	0.00325
SP2509	NA	chemical reagent	-2.771	2.79E-05	0.00444
MFSD2A	NA	transporter	2.949	2.89E-05	0.00444
JAK1/2	NA	group	-4.123	4.19E-05	0.0061

D-2-amino-5-phosphonovaleric acid	NA	chemical reagent	0.152	4.39E-05	0.0061
-----------------------------------	----	------------------	-------	----------	--------

Supplementary Table 8. Number of common DEGs identified by the FIN method in both scenarios considered for TCGA-GBM data. On average about 94% of the DEGs obtained when randomly selected subset was considered were also found in DEGs identified using the full TCGA-GBM dataset.

Scenario 2	Common DEGs	Total # DEGs	%common
Selection 1	5339	5665	94.25
Selection 2	5406	5697	94.89
Selection 3	5308	5645	94.03
Selection 4	5382	5710	94.26
Selection 5	5358	5722	93.64
Selection 6	5336	5743	92.91
Selection 7	5382	5684	94.69
Selection 8	5400	5797	93.15
Selection 9	5352	5720	93.57
Selection 10	5415	5698	95.03